JARO 03: 248–268 (2002)
DOI: 10.1007/s101620020028

JARO
Journal of the Association for Research in Otolaryngology

Dynamics of Noise-Induced Cellular Injury and Repair in the Mouse Cochlea

YONG WANG,[1,2] KEIKO HIROSE,[1,2] AND M. CHARLES LIBERMAN[1,2]

[1]*Eaton–Peabody Laboratory, Massachusetts Eye and Ear Infirmary, Boston, MA 02114, USA*
[2]*Department of Otology and Laryngology, Harvard Medical School, Boston, MA 02114, USA*

Received: 30 May 2001; Accepted: 24 October 2001; Online publication: 27 February 2002

ABSTRACT

To assess the dynamics of noise-induced tissue injury and repair, groups of CBA/CaJ mice were exposed to an octave-band noise for 2 hours at levels of 94, 100, 106, 112, or 116 dB SPL and evaluated at survival times of 0, 12, 24 hours or 1, 2, or 8 weeks. Functional change, assessed via auditory brainstem response (ABR), ranged from a reversible threshold shift (at 94 dB) to a profound permanent loss (at 116 dB). Light microscopic histopathology was assessed in serial thick plastic sections and involved quantitative evaluation of most major cell types within the cochlear duct, including hair cells (and their stereocilia), supporting cells, ganglion cells, spiral ligament fibrocytes, spiral limbus fibrocytes, and the stria vascularis. Morphometry allowed patterns of damage to be systematically assessed as functions of (1) cochlear location, (2) exposure level, and (3) postexposure survival. Insights into mechanisms of acute and chronic noise-induced cellular damage are discussed.

Keywords: acoustic trauma, permanent threshold shift, temporary threshold shift, histopathology

INTRODUCTION

Over the last 30 years, a good deal has been learned about which structures can be affected by acoustic injury, which are the most and least vulnerable elements, what is the nature of the damage at the structural and ultrastructural levels, which types of pathology dominate at short vs. long survival times, and which dominate at lower vs. higher level exposures (for review of the older literature see Saunders et al. 1985). In recent years, study of the mechanisms underlying noise-induced cochlear damage has begun to exploit the power of mouse genetics to manipulate gene expression in the ears of knockout and transgenic animals (e.g., Ohlemiller et al. 1999; Hakuba et al. 2000), and future expansion of work in this area is likely. Correspondingly, the histopathology of acoustic injury in the murine ear has received renewed interest (e.g., Ou et al. 2000a,b). However, the mouse ear remains much less well studied than that of, for example, guinea pig, chinchilla or cat. Thus, one aim of this study was to provide a comprehensive overview of the patterns of temporary and permanent noise-induced tissue damage in the mouse ear and to compare and contrast the damage patterns and associated functional losses with those reported in other mammalian models of acoustic injury. Such an overview is key in designing experiments in genetically modified animals. For example, the observation that profound noise-induced hearing loss (NIHL) in the mouse is routinely seen in the absence of significant hair cell loss constrains experiments designed to reduce NIHL by genetic manipulation of apoptotic pathways.

A challenging aspect of the study of acoustic injury is that the inner ear comprises a number of spatially distinct but functionally interdependent cellular systems, e.g., organ of Corti, spiral ligament, stria vascularis, and spiral limbus. Although the effects of noise on cells in each cellular system have been investigated, very few studies in any species have attempted

Correspondence to: Dr. M. Charles Liberman • Eaton–Peabody Laboratory • Massachusetts Eye and Ear Infirmary • 243 Charles Street • Boston, MA 02114. Telephone: (614) 573-3745; Fax: (617)-720-4408; email: mcl@epl.meei.harvard.edu

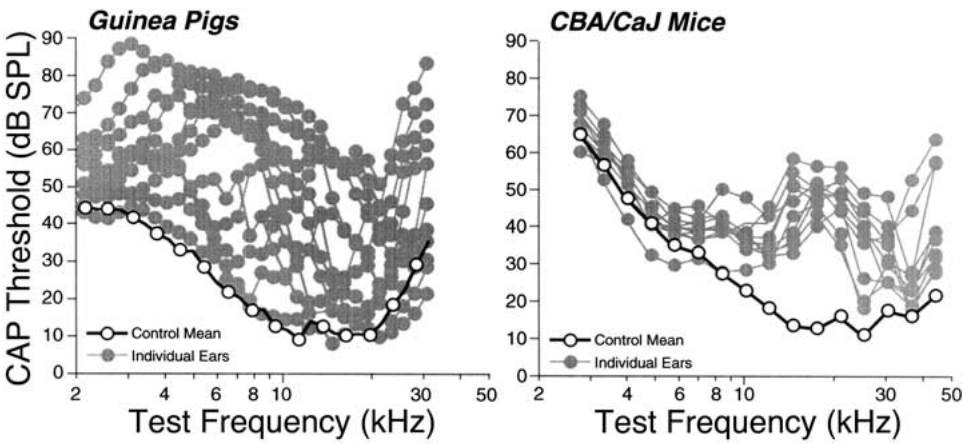

FIG. 1. Published data from our laboratory comparing the interanimal variability in the response to acoustic injury between albino guinea pigs (Hartley strain) and CBA/CaJ mice. The guinea pigs were all males (400–550 g) exposed to octave-band noise (4–8 kHz) at 109 dB for 4 h. Data are replotted from Maison and Liberman (2000). The mice were all males (23–29 g) exposed to octave-band noise (8–16 kHz) at 10 dB for 2 h. Data are replotted from Yoshida and Liberman (2000). The degree of threshold shift in each experiment was assessed by recording compound action potentials from the round window in response to tone pips at different test frequencies.

to inter-relate the damage patterns across all cell types in the same ears. Thus, a second aim of the present study was to address this issue by applying a histological processing technique for the mouse ear (Hequembourg and Liberman 2001) that allows a thorough, high-power, light microscopic analysis of all structures of the cochlear duct (which can be followed by detailed electron microscopic analysis of selected regions of the same tissue). Our evaluations identified many types of histopathology in several tissues, including the hair cells, nerve fibers, satellite cells in the spiral ganglion, the supporting cells of the organ of Corti, the fibrocytes in the spiral ligament and spiral limbus, and the stria vascularis. The explicit correlations of damage patterns among all the cellular systems of the inner ear suggest novel hypotheses as to the interactions among them in the response to noise and imply that increasing damage in one cell system can sometimes decrease the damage to another.

Another challenge in the study of the dynamics of tissue injury and repair in the inner ear after acoustic injury is the high degree of interanimal variability in the functional and structural changes seen among identically exposed animals (Bohne et al. 1999). The greater the interanimal variability in response to noise, the more difficult it is to reconstruct the natural history of the ear's response to noise from a series of histological snapshots taken at a series of postexposure survivals or following exposures of increasing intensity/duration. This type of variability has limited our understanding of issues such as how acute cellular events differ in cases where hair cells will ultimately degenerate compared with cases in which they will ultimately recover, or how long after an exposure do hair cells continue to degenerate, which cell types and structures are the primary targets of the acoustic exposure, which kinds of damage occur secondarily to these primary events, and how does damage in one structure affect the survival of other structures in the inner ear?

As illustrated in Figure 1, contemporaneous studies of acoustic injury in our laboratory show that interanimal variability in NIHL is roughly five times lower in the CBA/CaJ mouse than in the guinea pig, as might be expected given the greater genetic homogeneity in inbred strains of mice. In each experiment illustrated in Figure 1, groups of ~12 age-matched and sex-matched animals were exposed to octave-band noise designed to produce 35–40 dB of NIHL in the animal's midfrequency region. Although the noise bands and SPLs differed for mouse vs. guinea pig, the same noise-exposure facility was used, with the same calibration technique; thus, the control over variance in acoustic exposures was identical. In the particular examples shown, the mouse group showed a mean peak permanent threshold shift (PTS) of 38 dB (at 17.5 kHz) with a standard deviation of 4.06 dB. In contrast, although the mean peak PTS in the guinea pig group was almost identical (35.1 dB at 7.6 kHz), the standard five deviation was 21.33 dB, or roughly five times higher. In other studies of CBA/CaJ mice, we have seen comparably low variances in noise-exposed animals [e.g., peak PTS of 37.8 dB with a standard deviation of 3.62 dB in the control group from Yoshida et al. (2000)].

Thus, a third aim of the present study was to exploit this fivefold decrease observed in PTS variance in a mouse model of acoustic injury to gain insight into the dynamic processes of injury and repair via an experimental design in which groups of animals were exposed to the same noise band and sacrificed at different postexposure survivals for histopathological

analysis. To gain insight into the differences between reversible and irreversible damage, the sound pressure level of the exposure was varied across groups, producing a matrix of quantified observations in which damage patterns could be assessed as a function of exposure level and/or survival times. In all, 19 different exposure-level/survival-time groups were evaluated. Given the large number of groups to be assessed, the number of animals in each group was limited to four to allow a thorough histological evaluation. With such a small *n*, it is clearly not possible to assess independently the degree of interanimal variance in the present study. Rather, the aim of the histological analysis was to (1) evaluate qualitatively all structures of the inner ear, identify histopathology, and devise methods for quantification of these changes wherever practical, then, (2) attempt to gain insight into the dynamics of tissue injury and repair by evaluating these quantitative data as a function of cell type, cochlear location, survival time, and exposure level.

Analysis of the longitudinal patterns of noise-induced cellular pathology showed that damage to different tissues often occurred in characteristic, nonoverlapping cochlear locations. The existence of these complementary damage foci suggests fundamental differences in the underlying mechanisms of damage. Analysis of the damage patterns vs. time suggested which changes are reversible and showed that some types of degeneration continue for weeks after the exposure. Analyses of damage vs. exposure level showed some strikingly nonmonotonic relationships, suggesting that increasing damage in one structure can protect other structures from injury.

MATERIALS AND METHODS

Experimental groups and experimental design

Animals used in this study were CBA/CaJ mice obtained from Jackson Laboratories (Bar Harbor, ME) and entered into the study at 10 weeks of age. Animals were randomly assigned to one of a matrix of noise-exposure/survival-time groups or to a control group receiving no noise exposure. There were five control animals; all other group sizes are shown in Table 1. Except for groups with 0-h survival, cochlear function was tested in each animal via measurement of auditory brainstem responses (ABRs), and then cochlear tissues were fixed and harvested for histopathological analysis. For groups with 0-h survival, animals were perfused and cochlear tissues harvested immediately (<30 min) after noise exposure. All procedures were approved by the IACUC of the Massachusetts Eye and Ear Infirmary.

TABLE 1

Number of ears evaluated at each exposure level and survival

Exposure levels	*0 h*	*24 h*	*1 week*	*2 weeks*	*8 weeks*
94 dB		4		4	
100 dB	4	4		4	
106 dB	4	4	4	4	2
112 dB	4	4	4	4	
116 dB	4	4	4	4	4

Noise exposure

Mice were exposed to noise, unanesthetized and unrestrained, within cages suspended in a reverberant exposure box. The traumatic stimulus was a 2-h exposure to an octave-band noise (8–16 kHz). Noise levels in different groups varied from 94 to 116 dB SPL (Table 1). Exposure levels, measured at four positions within each cage, varied by <0.5 dB.

Anesthesia and surgical preparation

For either intravascular perfusion or ABR measurement followed by intravascular perfusion, mice were anesthetized with xylazine (20 mg/kg IP) and ketamine (100 mg/kg IP). For ABR measurements, surgical preparation involved only making a small slit in the pinna to better visualize the tympanic membrane. Only the right ear from each animal was tested.

ABR tests

ABR potentials were evoked with tone pips and recorded via needle electrodes inserted through the skin (vertex to ipsilateral pinna near tragus with a ground on the back near the tail). Stimuli were 5-ms pips (0.5-ms rise–fall with a $\cos^2$ onset envelope, delivered at 40/s). The response was amplified (10,000 ×), filtered (100 Hz – 3 kHz), and averaged with an A–D board in a LabVIEW-driven data acquisition system (National Instruments, Austin, TX). Sound level was raised in 5 dB steps from roughly 10 dB below threshold up to 80 dB SPL. At each sound level, 1024 responses were averaged (with stimulus polarity alternated). The software averager included an ''artifact reject'' feature in which response waveforms were discarded if the peak-to-peak voltage exceeded 15 μV. ABR ''threshold,'' defined as the lowest sound level at which the response peaks were clearly present, were read by eye from stacked waveforms obtained at 5 dB sound pressure intervals (up to 80 dB SPL). Thresholds typically corresponded to a level one step below that at which the peak-to-peak response amplitude began to rise.

Histological preparation

Animals were perfused intracardially with 2.5% glutaraldehyde and 1.5% paraformaldehyde in a 0.065 M phosphate buffer. Both petrous temporal bones were extracted and the round and oval windows opened to allow intralabyrinthine perfusion of fixative. After overnight postfixation in the same fixative at 4°C, cochleas were osmicated (1% OsO_4 in dH_2O) for 60 min and decalcified (0.1 M EDTA with 0.4% glutaradehyde) for 3 days. After decalcification, cochleas were dehydrated in ethanols and propylene oxide and then embedded in Araldite resins and sectioned in a roughly horizontal plane parallel to the spiral axis of the upper turn at 40 μM with a carbide steel knife. Sections were mounted in Permount on microscope slides and coverslipped. After light microscopic analysis, selected sections were floated off slides and remounted for ultrathin sectioning. For analysis in the electron microscope, these ultrathin sections were mounted on formvar-coated slot grids, stained with lead and uranyl acetate, and examined with a Philips CM10.

Morphometric analysis

For each case, the cochlear spiral was reconstructed in 3D using Neurolucida® (MicroBrightField, Colchester, VT) software and tracking the heads of pillar cells as the reference point for cochlear lengths. From these 3D data, the distance from the base was computed for each section through the duct using custom software. Cochlear location was converted into frequency, according to frequency map data described by Ehret (1983) which was fit to a mathematical equation:

$$f(\text{kHz}) = 3.109 * (10^{(100-d)*0.0142} - 0.7719)$$

where d is the percent distance from the cochlear base.

For a number of cochlear tissues, quantitative or semiquantitative protocols were devised to systematically assess severity of histopathology. For all semiquantitative analyses in which an arbitrary rating scale was employed, the test–retest reliability of the same observer was evaluated as well as the agreement between two different observers. Analysis of each histopathologic feature was performed in a concentrated fashion over consecutive days to minimize criterion drift. Unless otherwise stated, each cross section through the cochlear duct in each section was scored separately. For plotting purposes, data from each case were binned (bin width of 5% of cochlear length), averaged and normalized. The cochleas from the 8-week survival cases were processed during a different time period (by a different individual) and showed a higher level of mechanical artifact. For this reason they were not included in the quantitative analysis.

Hair cell counts. A standard cytocochleogram was prepared for each ear using high-power oil-immersion objectives and Nomarski optics. In each section through the cochlear duct, the number of present and absent hair cells was assessed throughout the entire section thickness. Evaluation of both the nuclear and cuticular regions was used to make these assessments.

Stereocilia analysis. Stereocilia on inner hair cells (HCs) can be well resolved in this material using Nomarski optics. For each case with 2 weeks of post-exposure survival, an observer estimated the fraction of stereocilia which were either lost, fused, or bent at more than a 30° angle from vertical. A modified quartile scale was employed: estimates of 90%–100%, 50%–90%, 10%–50%, and 0%–10% intact stereocilia were given scares of 1, 2/3, 1/3, and 0, respectively.

Spiral ligament fibrocytes. In every section through the cochlear duct, an observer estimated the percentage of fibrocytes in each class (type I, II, or IV) remaining. A quartile scale was employed (0%–25%, 25%–50%, 50%–75%, 75%–100% of cells remaining). Estimates of cell loss were performed with a 10X or 20X objective, were based on cell nuclei, and were referred to the cell density seen in control ears. Care was taken to assess each cochlear region separately because the detailed appearance of the spiral ligament changes dramatically from base to apex in all murine strains we have examined: CBA/CaJ, C57BL/6J, 129/SvEv, and FVB/N.

Spiral limbus fibrocytes. As for ligament fibrocytes, in every section through the cochlear duct, an observer estimated the percentage of limbic fibrocytes remaining. As the cells in the limbic central zone were harder to reliably assess than in the ligament, a cruder rating scale was employed: 0%–33%, 33%–66%, or 66%–100% remaining.

Vacuoles in the IHC area. The degree of vacuolization in the IHC area was assessed semiquantitatively via a rating scale in which absent, mild, moderate, and severe vacuolization were scored as 0, 1, 2, and 3, respectively. The observer was calibrated to the scale by first examining all the material without scoring in order to assess the range of histopathology possible. Mild vacuolization can be seen in some control ears, in a clear apex-to-base gradient. To normalize for this, all control ears were rated as well and average values of vacuolization vs. cochlear location for controls were subtracted from all experimental cases.

Stria vascularis. The cross-sectional area of the stria vascularis was measured in four cochlear regions. In each ear, sections representing the best cross sec-

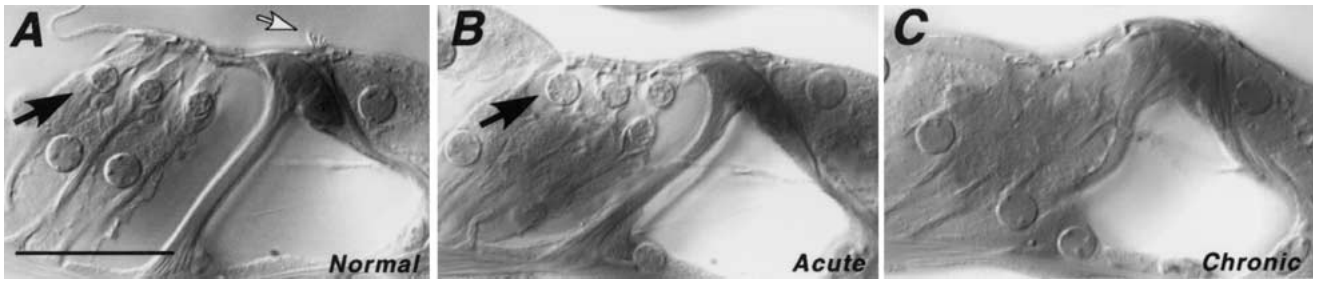

FIG. 2. Acute swelling of OHC nuclei 24 h after exposure to the noise band at 116 dB (**B**, arrow) in the region of the midbasal turn (~22 kHz region), in which all chronic ears (survivals ≥1 week after the 16 dB exposure) show complete selective loss of OHCs (**C**). Normal control cochlea at the same cochlear region (**A**) is shown for comparison. Note normal stereocilia bundle (open arrow) in control section. Scale bar in **A** (25 μm) applies to all panels. This and all subsequent digital micrographs underwent gamma adjustment and an unsharp mask filtering in Adobe Photoshop (Adobe Systems Inc., San Jose, CA) prior to submission.

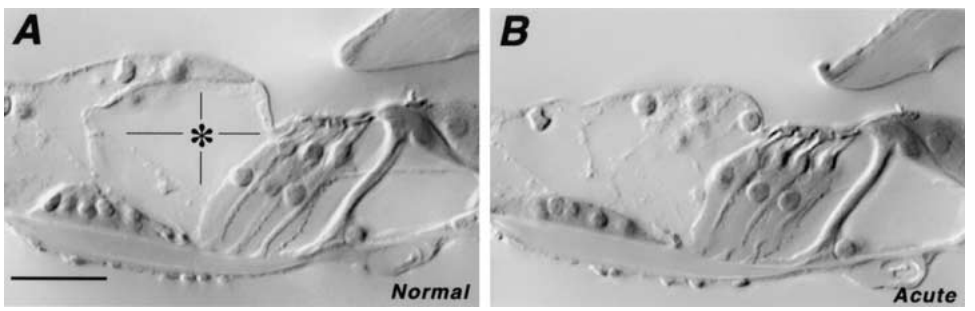

FIG. 3. Collapse of the Hensen cells and the outer space of Nuel (**B**) seen 24 h after noise exposure at 94 dB SPL. Normal space of Nuel (asterisk) and Hensen cells from the same region (midbasal turn) of a control ear are shown for comparison (**A**). Scale bar in **A** (25 μm) applies to both panels.

tion through each half-turn of the cochlear spiral were identified from the 3D reconstructions. In each of these sections, the stria was outlined via a drawing tube with a 20X objective and the cross-sectional area determined by computerized planimetry.

Spiral ganglion cells. The prevalence of vacuolated cells in the ganglion was determined by counting the total number seen with 100X oil-immersion objectives at all focal depths through an ideal cross section through each of the four half-turns of the mouse cochlear spiral. These counts were expressed as the percentage of cells affected by dividing the counts by the average number of ganglion cells seen in comparable cochlear regions of control ears.

Area of Nuel's space and Hensen cell height. These measurements were made only in the upper basal turn using a drawing tube and 100X Nomarski objectives. Only the ideal cross section was used in each case. Area and height were determined by computerized planimetry.

RESULTS

Overview of noise-induced histopathology in the mouse cochlea

Noise exposure in mouse, as in other mammalian models of acoustic injury, can lead to histopathology in virtually all structures of the cochlear duct, including hair cells and supporting cells of the organ of Corti, neuronal terminals and somata, fibrocytes in the spiral ligament and limbus, as well as cells of the stria vascularis. Before considering the quantitative analyses of these pathologies as a function of cochlear location, exposure level, and survival time, it is useful to present a qualitative overview of the nature of these changes as they appear in the murine cochlea.

A common pattern of hair cell damage was selective loss of outer hair cells (OHCs) with general preservation of supporting cell structure (Fig. 2C). This was typical in the lower basal turn at l–2 weeks after exposure to all levels ⩾100 dB. When similarly exposed ears were evaluated at acute survival times (0–24 h), OHCs in these regions showed swollen nuclei (Fig. 2B), positioned closer to the reticular lamina than normal. Severe nuclear condensation was also occasionally seen in these regions at 0–24 h postexposure (not shown). These dense, shrunken nuclear bodies were always surrounded by cytoplasmic and membranous debris.

Damage to stereocilia was widespread for all exposures ≥106 dB. In control cochleas (e.g., Figs. 2A and 3A), the IHC stereocilia were clearly visible using Nomarski objectives and optical sectioning. In noise-damaged ears, the stereocilia were often disarrayed or collapsed against the reticular lamina (Fig. 2B,C), in both acute (0–24-h survival) and chronic (1–2-week survival) cases.

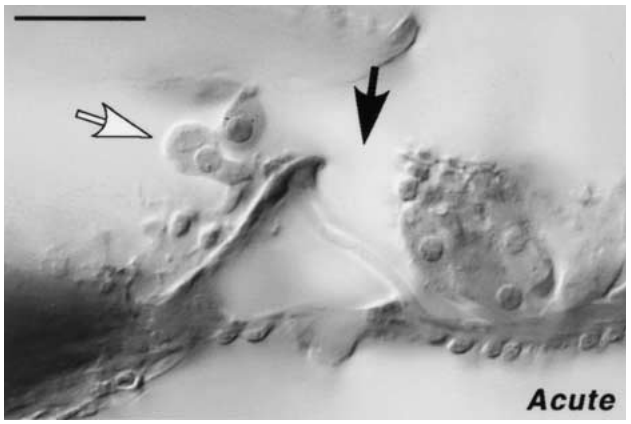

FIG. 4. Rupture of the reticular lamina (filled arrow) seen in acute ears (0–24 h) after exposure to the 116 dB noise band. Inner hair cells (open arrow) and other cellular debris in these areas are often displaced into scala media. Scale bar = 25 μm.

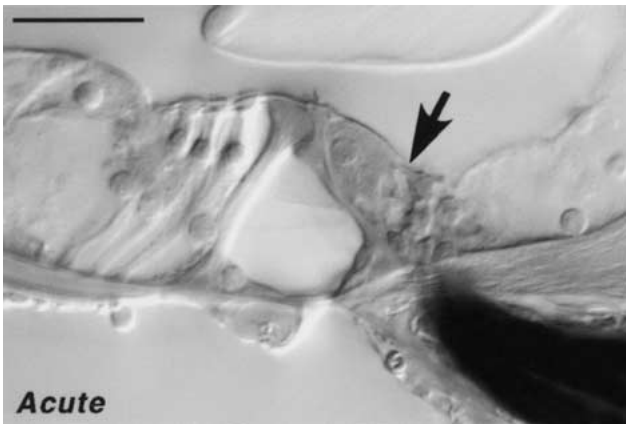

FIG. 5. Acute vacuolization in the IHC area seen immediately after a 106 dB exposure. Micrograph is from the upper basal turn. Scale bar = 25 μm.

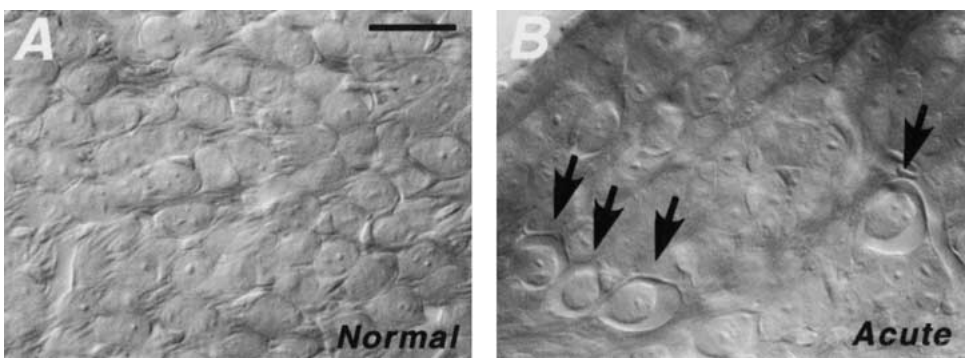

FIG. 6. Acute swelling of cells in the spiral ganglion (**B**, arrows) seen 24 h after a 112 dB exposure. Normal appearance of the spiral ganglion in control ears is shown for comparison in **A**. Both micrographs are from the upper basal turn. Scale bar in **A** (25 μm) applies to both panels.

Collapse of several types of supporting cells was common at both acute and chronic survivals. At all exposure levels there was acute collapse of the Hensen cells and the outer space of Nuel, which they enclose (Fig. 3A,B). At moderate sound levels there was buckling of pillar cells (Fig. 2C). At the highest exposure levels the reticular lamina was often acutely ruptured, with hair cell and other cellular debris floating in scala media (Fig. 4). These ruptures, which always occurred between outer pillar head and first-row OHCs, were patent as late as 1 week post exposure. At longer survivals, these disrupted regions resolved to a state in which the organ of Corti was replaced with a largely undifferentiated epithelium, although remnants of pillar cells were sometimes identifiable.

Damage to cochlear neurons was seen in both acute and chronic ears (Figs. 5, 6, and 7). At survivals ≤2 weeks, significant vacuolization was visible under the IHCs (Fig. 5). In electron microscopic studies, this phenomenon can be seen to represent swelling of unmyelinated terminals of IHC afferents (Liberman and Mulroy 1982; Robertson 1983). In short-survival cases, a significant number of swollen profiles were also seen in the spiral ganglion (Fig. 6B), whereas such profiles were rarely seen in control ears. Electron microscopic analysis suggests the myelinating satellite cells have swollen rather than the ganglion cells (Fig. 7). In regions of IHC loss, degeneration of peripheral axons and ganglion cells was first observed at survival times of 1 and 8 weeks, respectively.

Damage to fibrocytes was seen in both spiral limbus (Fig. 8) and spiral ligament (Fig. 9). In the ligament, type IV fibrocytes were the most vulnerable. In normal mice, this cell class is restricted to the basilar crest (Fig. 9A). After noise damage, a region of near-complete type IV loss (Fig. 9B) was visible for all exposure levels in the lower basal turn at 1–2-week survivals. There was no sign of regeneration of these cells in the 8-week animals. Loss of type I and II fibrocytes [normally concentrated in the spiral prominence region of the ligament (Spicer and Schulte 1991)] was also seen at higher exposure levels (≥112 dB). Degeneration of type III fibrocytes, which line the ligament next to the temporal bone, was never detectable. Loss of fibrocytes from the limbic central zone was common in middle and apical cochlear

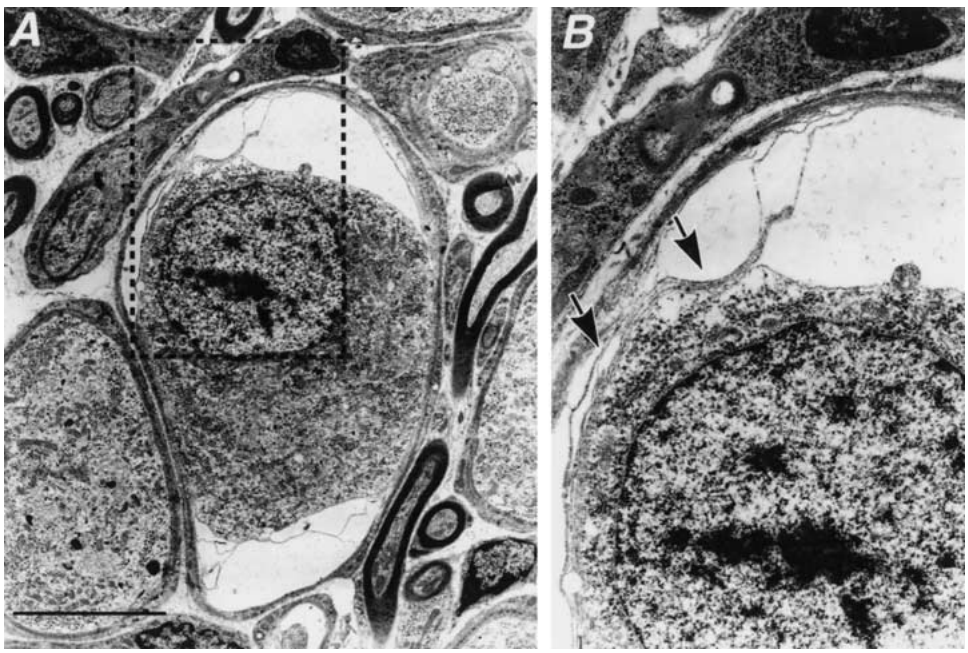

FIG. 7. Electron micrographs illustrating that the acute swelling in the spiral ganglion involves the satellite cells. One typical swollen cell complex is shown in **A**. The area of neuronal cytoplasm is reduced. One corner of the neuronal/satellite cell complex is shown at higher magnification in **B**, revealing that the myelin lamellae of the myelinating satellite cell are separated by large, fluid spaces (arrows) associated with a decrease in the size of the neuronal soma. Scale bar in **A** = 5 μm.

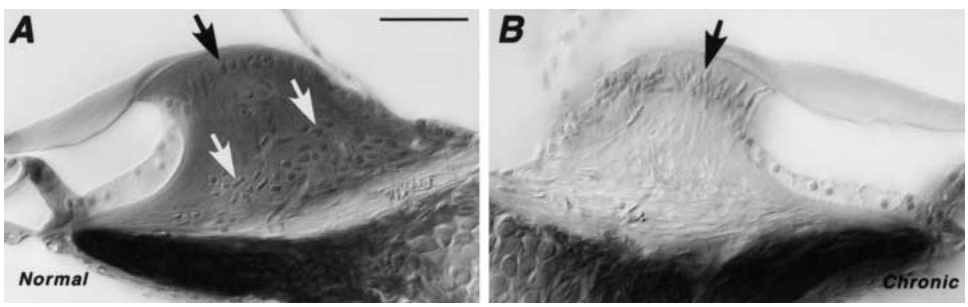

FIG. 8. Chronic acellularity of the limbic central zone (**B**) seen 2 weeks after exposure to the noise band at 112 dB SPL. For comparison, a normal-appearing limbus is shown in **A** in which clusters of fibrocyte nuclei are indicated by the white arrows. The interdental cells (black arrows) near the endolymphatic surface are apparently intact after the trauma. Scale bar in **A** (50 μm) applies to both panels.

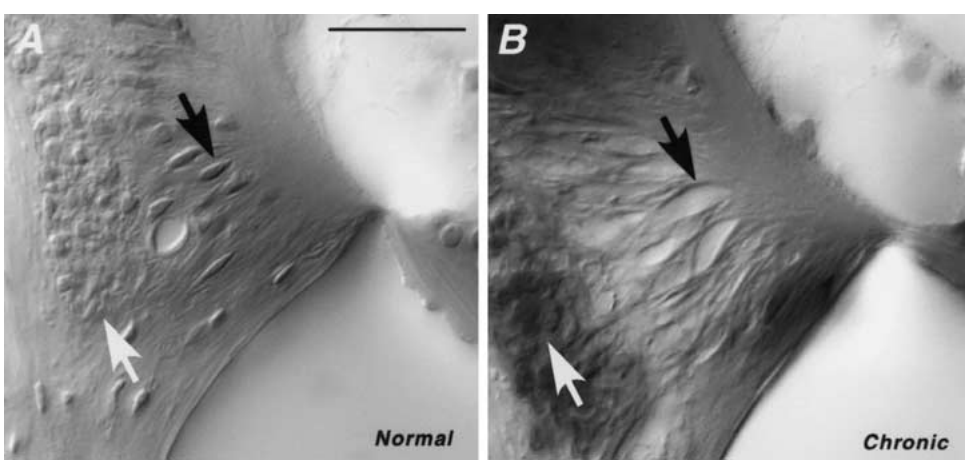

FIG. 9. Chronic degeneration of type IV fibrocytes in the spiral ligament seen following noise exposure. The case in **B** was evaluated 2 weeks after exposure to 94 dB SPL. The black arrow points to a hole in the collagenous matrix of the ligament where a type IV fibrocyte used to be. In the normal ear (**A**), a number of type IV fibrocytes (e.g., black arrow) are seen in the region of the ligament close to the attachment of the basilar membrane. The number of type III fibrocytes (white arrows) appears unaffected by the noise exposure. Both images are of the section from the midbasal turn. Scale bar in **A** (25 μm) applies to both panels.

regions. When present, this degeneration was virtually complete (Fig. 8A vs. 8B), leaving the interdental cells intact. The limbic cellular loss was accompanied by a decrease in the background staining of the limbic connective tissue.

Changes in the strial structure were noted in both acute and chronic ears. In these thick sections it was difficult to resolve cellular detail in the normal stria (Fig. 10A). Nevertheless, gross changes in strial volume and staining quality were clear, with extreme

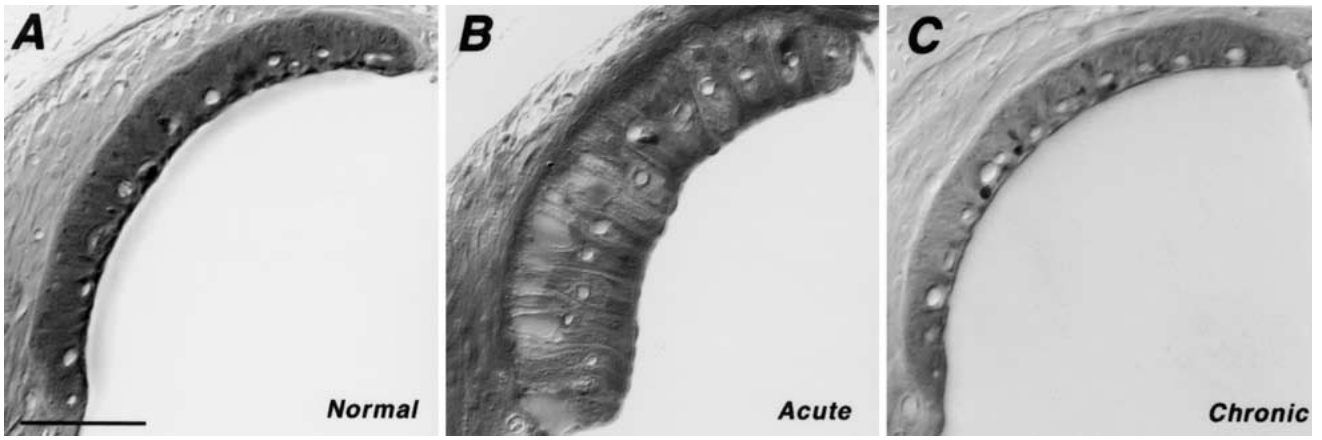

FIG. 10. Twenty-four hours after noise exposure, the stria is greatly swollen (**B**), whereas 2 weeks after the exposure, the diameter is slightly reduced (**C**). **B** and **C** are from the midbasal region of two cases exposed to the 116 dB noise band. **A** is from the same cochlear region of a control ear. Scale bar in **A** (50 μm) applies to all panels.

swelling characteristic of acute survivals (Fig. 10B). By longer survivals (2–8 weeks), the swelling has disappeared and shrinkage and some decrease in osmium staining were seen (Fig. 10C).

Inter subject variability within groups

Group size was typically four each cell in the matrix of exposure levels and survival times (Table 1), thus rigorous assessment of intersubject variability in these small groups is not feasible. Nevertheless, before turning to a consideration of mean group-by-group responses, it is instructive to consider individual responses in one representative group and how the variability may constrain interpretations.

For each animal, only the right ear was quantitatively assessed. The data in Figure 11 illustrate the typical degree of variability in ABR thresholds and patterns of hair cell loss and stereocilia damage among the four animals in one group. The group illustrated is that exposed to 112 dB SPL noise with 2 weeks of postexposure survival. The threshold shift pattern is that expected for a narrowband exposure, i.e., significant threshold shift for frequencies at and above the lower limit of the frequency band (8 kHz). Although all animals clearly show a precipitous high-frequency loss, the range of PTS at any one test frequency approaches 30 dB. The low variance for test frequencies at and above 12 kHz may reflect a saturation of the ABR metric: Survival of any population of high-threshold, broadly tuned neurons in the basal turn will insure a small high-threshold ABR response to a wide range of high-frequency test stimuli.

The cytocochleograms show that there is almost no IHC loss and that the degree of OHC loss is insignificant from apical to the lower basal turn. The overall pattern of OHC loss is similar across all four cases. Although the exact cochlear location of the lesion border varies by ~750 μm, one could say with some confidence that in evaluating similarly exposed animals sacrificed at earlier postexposure survivals, the OHCs in the basal 1–2 mm of the spiral are destined to degenerate.

The analysis of stereocilia damage also shows a similar pattern in each of the four ears. In each case there is a sizable region of the upper basal turn over which more than 75% of the IHC stereocilia has been destroyed, disarrayed or fused. In three of the four cases, the pattern is very similar; in a fourth case (309), the damage has spread further apically than in the other three. Again, although there are clearly intragroup differences, it appears highly likely that ears exposed at this SPL will show severe chronic stereocilia disarray.

Damage vs. cochlear location frequency

The longitudinal patterns of histopathology clearly show that different cell types are damaged in different cochlear regions, both for acute changes seen at 24 h (Fig. 13) and chronic changes seen 2 weeks postexposure (Fig. 12).

Considering first the patterns of threshold shift vs. frequency, the ABR data show that the highest exposure level (116 dB SPL) resulted in profound and widespread PTS, with a complete lack of ABR responses at all test frequencies up to the highest test levels (80 dB SPL), even at 2 weeks postexposure (Fig. 12). At the other extreme, the lowest exposure level (94 dB SPL) produced 45 dB peak shift in group mean thresholds when assessed at 24 h postexposure (Fig. 13). However, this largely temporary threshold shift (TTS) resolved to a minimal PTS (<10 dB) when assessed at 2 weeks (Fig. 12). When the peak threshold shift (TS) was <50 dB, maximal losses were seen at test frequencies of

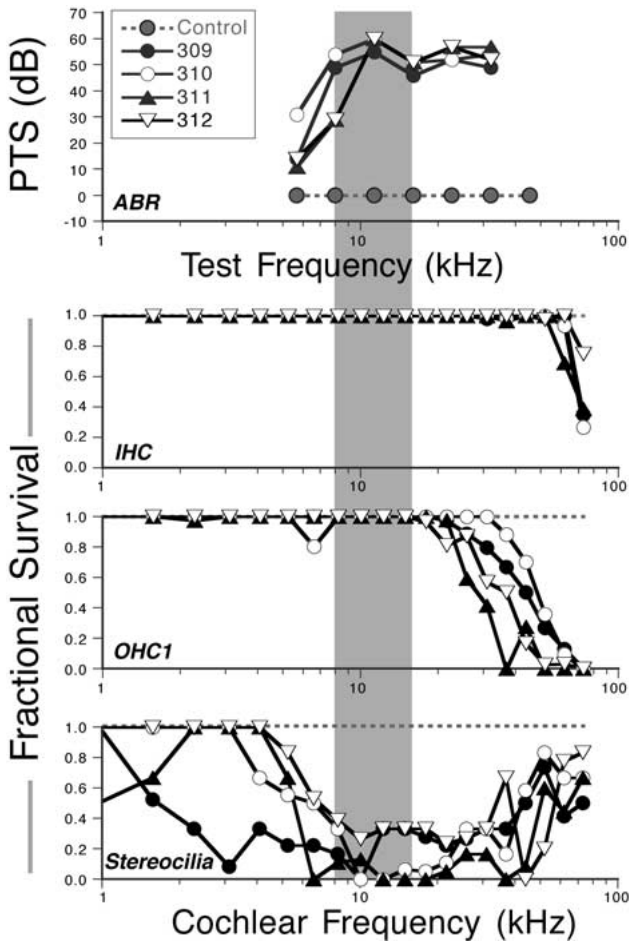

FIG. 11. ABR thresholds (top panel), stereocilia analyses (bottom panel), and cytocochleograms (middle panels) from each of the four ears exposed to the 112 dB noise band and evaluated at 2 weeks postexposure illustrate typical within-group variance. ABR thresholds are expressed as permanent threshold shift (PTS), i.e., dB re mean values at each test frequency for the unexposed control group ($n = 5$); for the control group the standard errors at each test frequency are between 1.2 and 1.8 dB. Stereocilia condition was assessed on IHCs only (for details, see Methods). Cytocochleograms represent complete hair cell counts from serial sections. Cochlear locations are divided with a bin width corresponding to 5% of total cochlear length, and all values within each distance bin are averaged in each case. For OHCs, only first-row (OHC1) data are shown. The damage is most severe in this row, and the variance is representative of that in the other two rows. The key in the top panel identifies the animal ID numbers in this group and applies to all panels. The gray box indicates the bandwidth of the traumatizing stimulus.

16 kHz (100 dB at 2 weeks) or 22 kHz (94 dB at 24 h). This upward shift of the maximal loss *re* center of the exposure band is typical of acoustic injury (Cody and Johnstone 1981; Liberman and Mulroy 1982).

Chronic histopathology (Fig. 12). With respect to IHC loss, mean cytocochleograms at 2-week survival showed two foci of hair cell loss: one in a region tonotopically appropriate to the exposure band and one in the extreme base, or "hook," region of the cochlea. Control cochleas ($n = 5$) show no comparable loss of hair cells in either location. In the region of the tonotopic focus, the IHC loss (seen only at 116 dB) was associated with nearly complete loss of all supporting structures of the organ of Corti.

The existence of dual damage foci following narrow band exposure, one tonotopic and one in the hook, has been noted in previous studies of acoustic injury in other animal models (Fried et al. 1976; Liberman and Kiang 1978). The OHC loss pattern similarly showed only a hook focus at the lower exposure levels. However, at 116 dB the OHC loss covered the entire basal turn rather than showing two separate foci. For simplicity, only first-row OHC data are shown in Figure 12; however, the second and third rows show analogous patterns.

A similar pattern of damage was seen for IHC stereocilia (OHC stereocilia are too small to be reliably resolved at the light microscopic level). At the two lowest exposure SPLs, clearcut damage was restricted to the extreme base. At 106 dB, a peak of stereocilia damage appeared precisely at the tonotopic focus. When the level reached 112 and 116 dB, the damage spread to encompass virtually the entire basal half of the cochlea.

A markedly different longitudinal pattern of damage was seen for spiral ligament fibrocytes. For all exposure-level groups, type IV fibrocytes were consistently destroyed in a cochlear region complementary to that seen for IHCs, i.e., the region between the tonotopic and hook foci of IHC damage. Loss of type II fibrocytes in the ligament showed a similar longitudinal pattern; however, the degeneration was clearcut only in the ears exposed to 116 dB SPL (data not shown).

The fibrocytes in the spiral limbus showed a less consistent damage pattern. At 106 dB, one out of four animals showed limbic degeneration; the locus in that case extended apically from the tonotopic focus. At 112 dB, all four cases showed a discrete region of acellularity coincident with that of the tonotopic IHC focus. Surprisingly, none of the ears in the 116 dB group showed any limbic degeneration at all. This nonmonotonic behavior is discussed below.

Quantitative analysis of the cross-sectional area of the stria vascularis showed consistent shrinkage at 2-week survival. At the lower exposures (94 and 100 dB SPL), the changes were restricted to the middle two measurement points (spanning the tonotopic focus). At the higher SPLs, the pathology spread apically and basally; however, the changes were always minimal at the extreme base, near the hook focus.

Acute histopathology (Fig. 13). There are similarities and differences in the longitudinal patterns of his-

topathology in the 24-h survival groups with respect to those described above for the 2-week survival.

With respect to hair cell damage patterns, tonotopic and hook foci are evident but appear in a different form. The cytocochleograms in Figure 13 show OHC loss in the hook following all exposures ≥100 dB. The tonotopic focus is not evident in the acute IHC cytocochleograms: At levels of 112 dB and below, there was no significant hair cell loss in this region. However, among ears exposed to 116 dB, the region of the tonotopic focus showed rupture of the reticular lamina in three out of four cases. As illustrated in Figure 4, this condition leaves hair cell remnants floating free of the organ of Corti, making hair cell counts difficult. As shown by comparing Figures 12 and 13, the cochlear location of the reticular lamina rupture at 116 dB after 24 h is identical to that of the tonotopic focus of IHC loss for 116 dB after 2 weeks.

Fibrocyte pathology in the spiral ligament had not appeared by 24 h, thus no quantification was made. Fibrocyte damage in the spiral limbus, on the other hand, was just detectable at this survival and appeared at similar exposure levels and cochlear locations to those affected in the survival data.

Damage to the stria vascularis at 24 h took the form of swelling of the cross-sectional area. As quantified in Figure 13, this swelling was detectable at all exposure levels at and above 100 dB and was widespread along the cochlear spiral.

Two types of neural damage were evident 24 h after all exposure levels: vacuolization under the IHCs (Fig. 5) and swollen satellite cells in the spiral ganglion (Figs. 6 and 7). In general, both forms of damage peaked in the region immediately basal to the tonotopic focus, especially at the two lower exposure levels (94 and 100 dB). The degree of vacuolization was more striking at 0 h (see below). Note that these patterns are similar to the frequency pattern of TTS seen in the same animals, especially for the 94 dB group. At the two higher exposure levels,

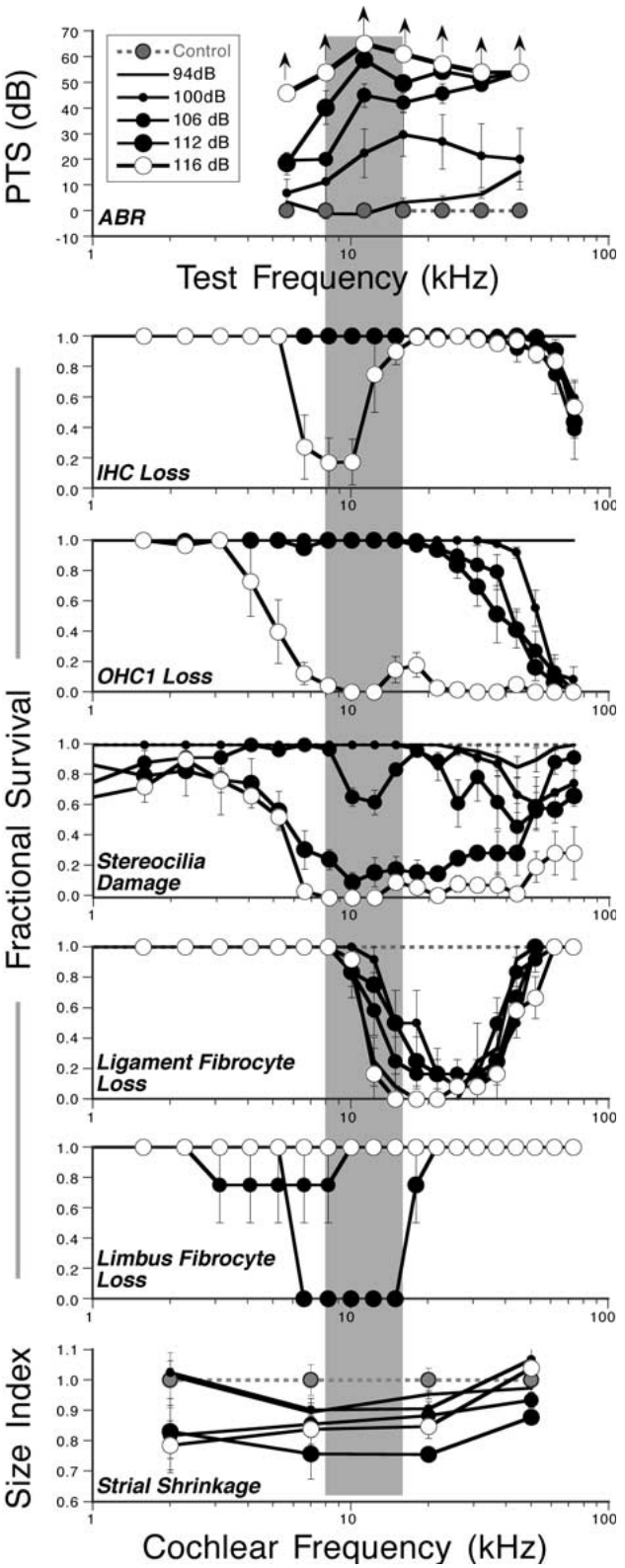

FIG. 12. Summary of the longitudinal patterns of permanent damage seen at 2 weeks postexposure. Data from all five exposure levels are summarized in these panels, as indicated by the symbol key in the top panel. In each panel, data from all four ears from each exposure group have been averaged and the means (±SEM) are shown. ABR thresholds are expressed as permanent threshold shift (PTS), i.e., dB re mean values at each test frequency for the unexposed control group ($n = 5$); for the control group the standard errors at each test frequency are between 1.2 and 1.8 dB. In the middle five panels, the symbols for Control ears have been eliminated to preserve clarity. However, no hair cell loss was seen in these ears and the condition of the other cell types is normal by definition (See Methods for details on quantification procedures for all cell types). The gray box indicates the bandwidth of the traumatizing stimulus. The arrows in the ABR panel (top) indicate that the values have reached the maximum measurable PTS, which corresponds to the difference between 80 dB SPL and the mean control thresholds at that test frequency. SPL was limited to 80 dB in the ABR tests to prevent additional acoustic injury.

the prevalence of swollen cells increased in the 8 kHz region; however, the maximum effects were still seen in the 22 kHz region.

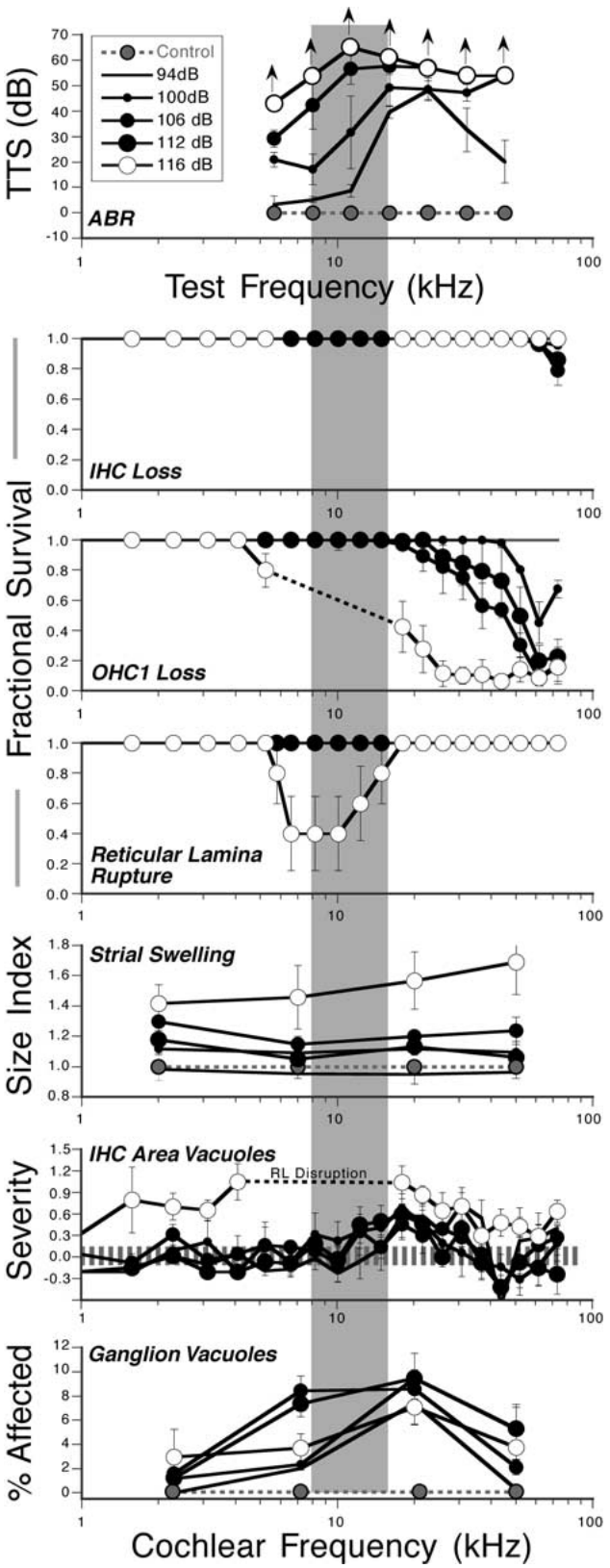

Damage vs. exposure level

Chronic histopathology (Fig. 14). The growth of PTs with exposure level in the CBA/CaJ mouse is monotonic (Fig. 14). At the peak frequency (22.6 kHz), the growth rate on the steepest part of the curve (between 94 and 106 dB exposures) corresponds to an increase of ~3.5 dB of PTS for every 1 dB increase in exposure level, as seen in previous reports (Yoshida et al. 2000). The growth rate at 8 kHz test frequency is somewhat lower (~2.25 dB PTS/dB exposure level).

Data in the remaining panels of Figure 14 show that the growth of chronic cellular damage with exposure level can show fundamentally different patterns, depending on cell type and/or cochlear location. Some are monotonic, others are nonmonotonic, and several of the graphs suggest an abrupt change in behavior at 116 dB SPL, the exposure level at which acute rupture of the reticular lamina occurred.

Monotonic behavior was seen for hair cell loss, stereocilia damage, and collapse of Hensen cells. Hensen cell collapse was the simplest in the sense that the degree of collapse increased systematically with exposure level. Although damage to hair cells and stereocilia also grew monotonically with exposure level, hair cell loss increased dramatically at 116 dB whereas stereocilia damage grew markedly at 112 dB exposures. The chronic collapse of the Nuel space also appeared suddenly at 116 dB.

The degeneration of the limbic fibrocytes followed a fundamentally different (nonmonotonic) pattern: The damage grew dramatically from 100 to 112 dB exposures and then disappeared at 116 dB. Strial shrinkage also showed slight improvement at 116 dB, whereas it steadily worsened from 94 to 112 dB. After the 94 dB exposure, the only clearcut histopathology was in the type IV fibrocytes and possibly the stria vascularis.

Type IV fibrocyte degeneration showed a third type of pattern. Cell loss appears to have saturated at the lowest exposure used; degree of damage at 116 dB was not significantly worse than that seen at 94 dB.

Acute histopathology (Fig. 15). The data in Figure 15 summarize the growth of TTS and acute cellular damage (i.e., 24 h postexposure) with exposure level. The ABR data show orderly monotonic behavior of TTS at the 8 kHz test frequency with a growth slope

FIG. 13. Summary of the longitudinal patterns of acute damage seen at 24 h post exposure. Data from all five exposure levels are summarized, as indicated by the symbol key in the top panel. Cytocochleograms and IHC area vacuole analysis are incomplete for the 116 dB group (open circles) in midcochlear regions because fracture of the reticular lamina and massive disruption of the tissue organization made it difficult to score. All other conventions for data display are as described for Figure 12.

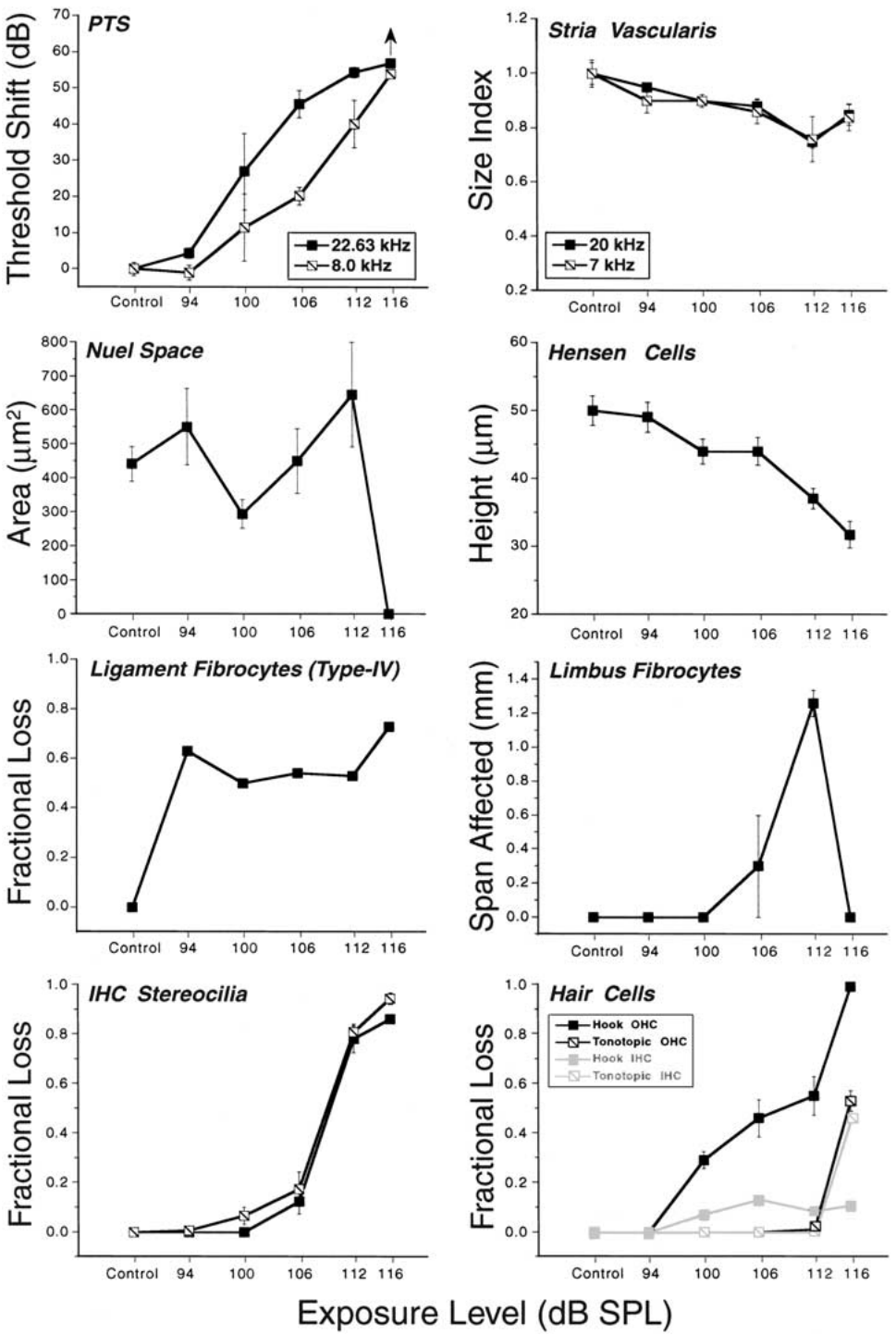

FIG. 14. Summary of the relations between exposure level and PTS (top panel) or degree of chronic histopathology at 2 weeks postexposure in different tissues (6 lower panels). In each panel, mean data (± SEM) are shown from all four ears in each exposure level group. **PTS:** PTS data at two frequencies are replotted from the same database used for Figure 12. **Stria vascularis:** As described in Methods, the cross-sectional area of the stria was measured in each ear in the middle of the upper-basal (20 kHz region) and lower-apical (7 kHz region) half-turns. All values were normalized with respect to the mean values from control ears at the appropriate cochlear location. **Nuel Space** and **Hensen Cells:** Measurements were made in each ear from the middle section through the upper-basal half-turn (the 20 kHz region) to provide the best cross-sectional view. Nuel space was defined as shown in Figure 3A. Hensen cell height was defined as the maximum height from the basilar membrane along a line perpendicular to the basilar membrane. **Type IV Fibrocytes:** In each ear, the values obtained for fractional survival (See Methods) were averaged over all cochlear regions spanning the 10% and 60% distance points (corresponding to the 9.0 to 56 kHz regions). **Limbus Fibrocytes:** In each ear, the cochlear distance over which there was complete degeneration of limbic fibrocytes was determined. **IHC Stereocilia:** In each ear, the values for stereocilia damage were averaged over a span corresponding to 15% of total cochlear length, and centered on either the 20 or the 7 kHz region, as noted in the key. **Hair Cells:** In each ear, the values for fractional hair cell survival were separately averaged for IHCs and first-row OHCs, and separate values were computed for the hook focus (defined as all cochlear regions basal to the 20 kHz point) and the tonotopic focus (defined as all cochlear regions between the 5 and 20 kHz points).

(~4 dB TTS/dB exposure) similar to that seen for PTS. At 22.6 kHz, the TTS has essentially saturated at the lowest exposure SPL.

The patterns of cellular damage show both monotonic and nonmonotonic behavior. As with the chronic changes, Hensen cell collapse systematically worsened with increasing exposure level, and the Nuel space showed a precipitous collapse when SPL reached 100 dB. Strial edema showed a dramatic worsening at the 116 dB exposure level. Both types of

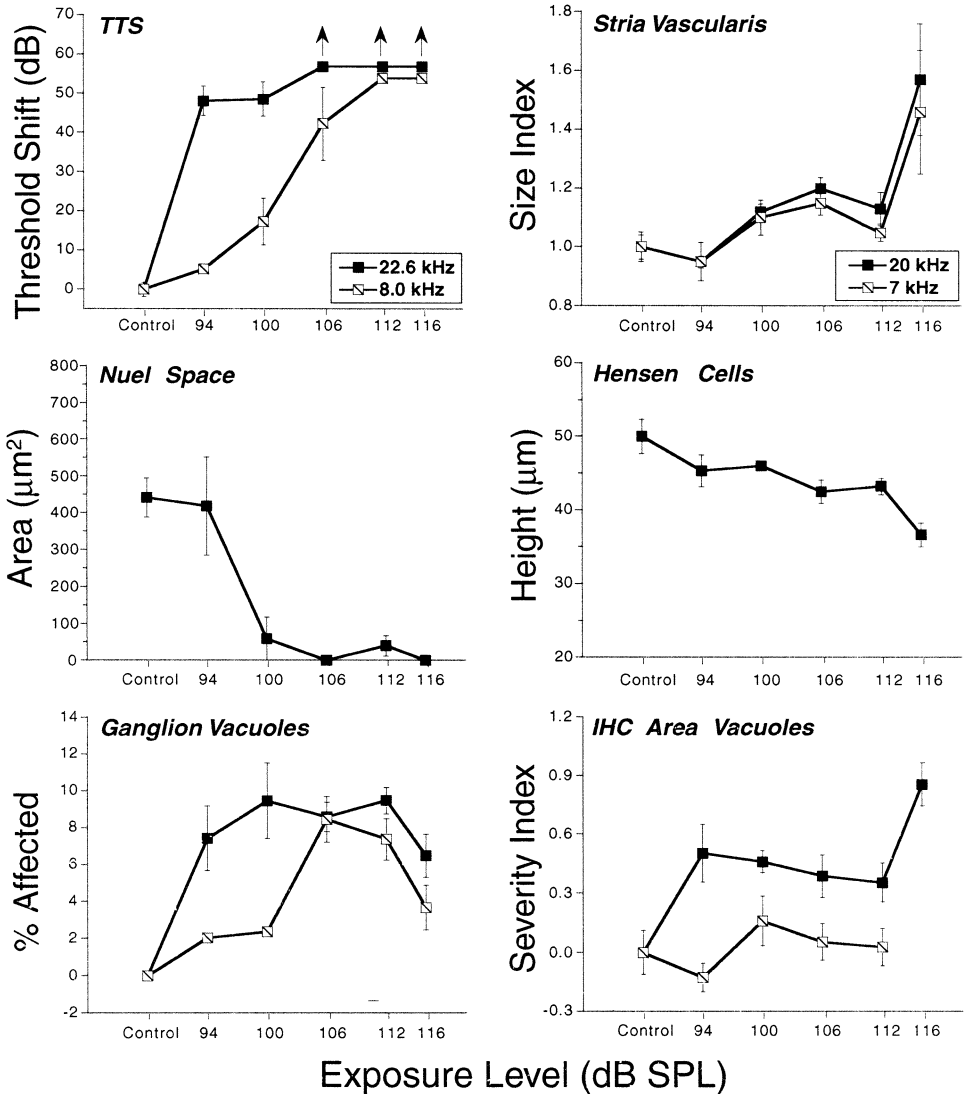

FIG. 15. Summary of the relations between exposure level and temporary threshold shift (top panel) or degree of acute histopathology at 24 h postexposure in a number of different tissues (four lower panels). Derivation of all data points and conventions for data display for all other panels are as described for Figure 14, except as follows. **Ganglion:** As described in Methods, the number of swollen cells was measured at the middle of the upper basal (20 kHz region) and the lower apical (7 kHz region) turns of each case. This number was divided by the average number of cells seen in analogous sections in control ears. **IHC Area Vacuoles:** In each ear, the values for degree of vacuolization were averaged over a span corresponding to 15% of total cochlear length and centered on either the 20 or the 7 kHz region, as noted in the key.

neural swelling grew nonmonotonically with exposure level. The prevalence of swelling in the spiral ganglion clearly decreased at the 116 dB exposure. The vacuolization in the IHC area showed a complex behavior, with severity slightly decreasing in both cochlear regions after peaking at either 94 or 100 dB exposures.

Damage vs. time

Examination of the progression of damage vs. time provides insight into both recovery processes and the time course over which degeneration continues after acoustic insult.

Issues relevant to recovery of function are summarized in Figure 16. There was extensive recovery of thresholds at 22 kHz (summarized in the upper-left panel) between 24 h and 2 weeks after 94, 100, and 106 dB exposures but not after 112 and 116 dB (Fig. 16, top left). The lack of recovery at the highest exposure levels is probably due, in part, to constraining test tones to SPLs ≤80 dB. Only at 94 dB was the threshold shift largely reversible.

The remaining panels of Figure 16 document all the morphological measures at the 22 kHz (upper basal turn) location which showed "improvement" over the same time frame. Reformation of the space of Nuel was almost complete for the 100, 106, and 112 dB exposures: 94 dB exposures never produced significant collapse in the acute phase, and no recovery was seen after the 116 dB exposures. The Hensen cell collapse recovered only for the 94 dB exposure; other exposures either showed no significant change or continued further collapse between 1 day and 2 weeks postexposure. Swelling in the spiral ganglion developed over the first 24 h and was completely reversible at all exposure levels, with few swollen profiles seen at 1 week and none at 2 weeks postexposure. In contrast to the ganglion abnormalities, neuronal vacuolization in the IHC area peaked immediately after the exposure and, by 2 weeks, had

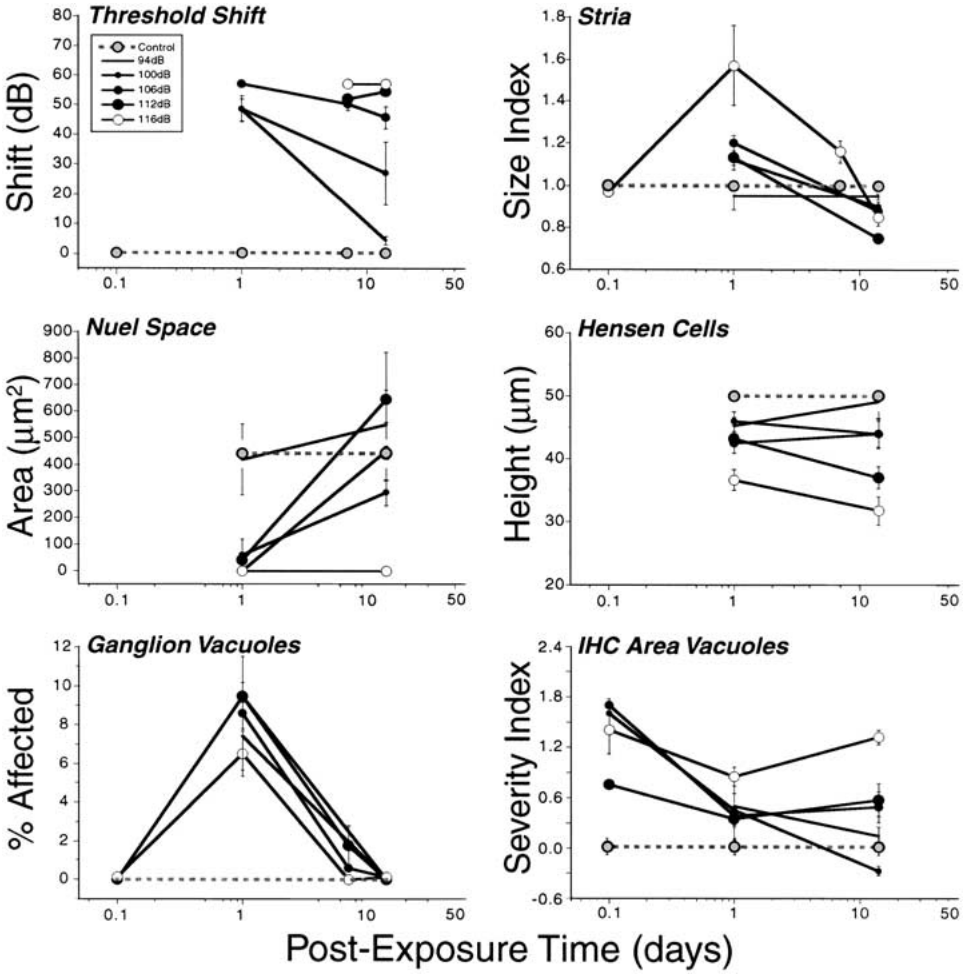

FIG. 16. Summary of the relations between postexposure time and threshold shift (top panel) or degree of histopathology in a number of different tissues (lower four panels). All conventions for data extraction and display are as described for Figures 14 and 15.

recovered only for the two lowest exposure SPLs (94 and 100 dB). Strial edema was absent by 2 weeks postexposure; however, it resolved to significant strial shrinkage.

Ongoing degeneration of cellular structures was seen among the fibrocytes (in both limbus and spiral ligament), spiral ganglion cells, and hair cells. The continuing loss of hair cells is quantified in Figure 17, where the mean fraction of OHCs missing in the hook lesion focus (cochlear regions basal to the 22 kHz point) is plotted vs. postexposure survival. Immediately after the exposure, all OHCs are present, although there is severe nuclear swelling in this region (Fig. 2B). Significant OHC loss continues for 2 weeks postexposure, and the lack of clear saturation suggests that loss may continue beyond the 2 week point.

Massive degeneration of type IV fibrocytes in the ligament occurred between 1 day and 1 week after exposure. Fibrocytes looked normal at 24 h, and although the degeneration had begun by 1 week, cell loss was not widespread until 2 weeks. Degeneration of limbic fibrocytes followed a more accelerated time course as early-stage degeneration was clear at 24 h. Comparison of the data in Figures 12 and 13 suggests that degeneration continues between 24 h and 2 weeks postexposure.

Loss of peripheral axons and spiral ganglion cells was seen only at 116 dB exposures and only in the tonotopic focus where IHC loss was widespread. Degeneration of peripheral axons was first observed at 7 days, and loss of cell bodies was first observed at 8 weeks. Neuronal degeneration and loss in the hook focus was difficult to assess, as IHC loss was subtotal and restricted to the basalmost section through the organ of Corti.

DISCUSSION

Functionally important structural changes: TTS vs. PTS

Comparing patterns of threshold shift with patterns of histopathology allows inferences to be drawn regarding the functionally important structural changes underlying noise-induced hearing loss. Existing literature on acoustic injury in nonmurine animal models suggests that the changes underlying TTS and PTS

are fundamentally different, thus the two are considered separately.

Temporary threshold shifts: TTS. The 94 dB exposures are particularly relevant to the issue of temporary/reversible threshold shift since this sound level led to a ~50 dB peak threshold shift at 24 h, which recovered almost completely by 2 weeks postexposure. As such, it represents a severe form of TTS, just at the border of full reversibility. Several higher-level exposures showed threshold recovery; however, at 100 dB and higher, there was significant PTS in the final steady state.

In other animal models of acoustic injury, several types of structural change have been suggested as important contributors to the reversible components of noise-induced hearing loss. These include (1) changes in the stereocilia bundle, including disarray (Mulroy and Whaley 1984), loss of tip links (Zhao et al. 1996; Husbands et al. 1999), or depolymerization of rootlets (Liberman and Dodds 1987); (2) excitotoxic effects on neural elements in the IHC area manifested as extreme swelling of peripheral terminals (Spoendlin 1971; Liberman and Mulroy 1982; Robertson 1983); (3) collapse of the supporting cells in the organ of Corti including both pillar cells (Nordmann et al. 2000) and Hensen cells (Flock et al. 1999); and (4) strial edema (Santi and Duvall 1978). It is not unlikely that all these changes make some contribution to threshold shift, depending on the severity of the exposure and the species involved. Each of these four major types of damage was seen in the present study.

Stereocilia condition was not assessed quantitatively at acute survival times; however, qualitative analysis suggests that the chronic pattern of stereocilia damage (Fig. 12) was visible immediately after the exposure and did not significantly recover with time. Thus, although stereocilia loss, disarray, and fusion are acute manifestations of acoustic injury, they do not appear to be reversible and thus constitute the permanent components of a compound threshold shift. Consistent with this view is the observation that stereocilia condition appeared normal at all survival times following the 94 dB exposures, which caused only a TTS.

Strial edema has been noted in some previous studies of acute acoustic injury; however, its contribution to TTSs remains poorly understood. In the present study, strial edema was shown to be an important and consistent sequela of acoustic overexposure. However, it was not reversible in the sense that every exposure level with significant edema at acute stages (SPL ≥ 100 dB) showed significant shrinkage at chronic stages. Furthermore, edema was NOT detectable after the 94 dB exposure (Fig. 13), which, as discussed above, corresponds to a very severe TTS, just at the limit of full functional reversibility.

Putative excitotoxic effects included satellite cell swelling in the ganglion and vacuolization in the IHC area corresponding to swelling of afferent terminals (see the subsection "Complementary lesion foci" below for further discussion of possible mechanisms of excitoxicity). Although both pathologies were seen acutely after all exposures, terminal swelling was better correlated with the measured TTS. Although both longitudinal patterns were consistent with the frequency region of maximum TTS, especially for the 94 dB exposure (Fig. 13), the immediate appearance and monotonic recovery of IHC vacuolization, at least following the 94 and 100 dB exposures (Fig. 16), was more consistent with the time course of threshold shift and recovery than the delayed appearance of the satellite cell swelling (Fig. 16). Although kainate-induced swelling of dendrites has been shown to recover with a similar time course as the recovery of ABR responses (Zheng et al. 1997), evidence that swelling of afferent dendrites is not the functionally important change in this type of noise-induced TTS comes from a study in which these excitoxic effects were blocked pharmacologically without changing the degree of TTS (Puel et al. 1988). Furthermore, the functional consequences of these excitotoxic effects are constrained by the fact that only a subset of neurons appear to be affected.

For example, no more than 15% of ganglion cells were swollen in any section (Fig. 15); and previous ultrastructural studies of noise-induced terminal swelling suggest that fewer than half of the terminals are affected when the threshold shift is reversible (Liberman and Mulroy 1982). Data from other types of cochlear pathology show that loss of <50% of neural elements causes threshold shifts of <6 dB (Liberman et al. 1997). Thus, to postulate that these excitotoxic changes are responsible for 40–50 dB of TTS requires the further assumption that synaptic transmission is impaired in most of the neurons which appear normal at the light or electron microscopic levels.

Changes in supporting cell structure almost certainly contribute to the reversible components of threshold shift observed in this study. In acute ears (24-h survival), there was collapse of the outer space of Nuel associated with a buckling of the arching portion of the Hensen cells and a decrease in height of the organ of Corti (Figs. 3, 14, and 15). The collapse of Nuel space recovered significantly by 2 weeks after all exposures except 116 dB, but the height of the Hensen cells recovered completely by 2 weeks only for the 94 dB exposure (Fig. 16). This change in architecture is similar to that reported in an *in vitro* study of the guinea pig cochlea in which the sensory

epithelium was observed in response to simulated acoustic injury (Flock et al. 1999). In this isolated hemicochlea preparation, a reversible collapse of the Hensen cell and outer space of Nuel was correlated with reversible changes in microphonic potentials. Such dramatic changes in supporting cell architecture would be expected to change cochlear micromechanics and thus cochlear sensitivity. Others have suggested that pillar collapse is an important component of reversible noise-induced hearing loss in chinchilla (Nordmann et al. 2000). Our studies in mouse do not support this view: Although pillar collapse was seen (e.g., Fig. 2C), it was not obvious to visual inspection at any but the highest exposure levels. Thus, although pillar collapse may be partially reversible, in the mouse ear pillar collapse is not seen until sound pressure levels which result in profound permanent loss are reached.

Permanent threshold shifts: PTS. Previous studies of chronic acoustic injury have documented that most structures of the cochlear duct can be damaged by sound if the exposure level is raised sufficiently. Previous reports have described hair cell loss, neuronal loss, stereocilia damage, and supporting cell collapse, as well as loss of fibrocytes in the limbus and lateral wall and strial degeneration (for review, see Saunders et al. 1985). All of these phenomena were also seen in the present study.

Past studies attempting to identify the functionally important permanent structural changes after acoustic injury have concluded that (1) the most vulnerable elements of the cochlear duct are the hair cells (Liberman and Kiang 1978); (2) most of the noise-induced PTS can be well accounted for by loss of hair cells and/or damage to the stereocilia (Liberman and Dodds 1984); and (3) ears with PTS > 40 dB can show no loss of hair cells and no light microscopic histopathology in the entire cochlear duct besides damage to the hair cell stereocilia (Liberman and Dodds 1984).

Data from the present study are consistent with the view that the most functionally important structural change underlying PTS is damage to or loss of stereocilia: (1) Minimal hair cell loss was seen in regions with profound PTS, and (2) when PTS exceeded ~40 dB, the longitudinal pattern and degree of stereocilia damage correlated well with the frequency range and degree of PTS (Fig. 12). In the present study, only the IHC stereocilia were assessed. Nevertheless, in other analyses of noise-induced stereocilia damage, damage to OHC stereocilia (especially those in the first row) is almost always worse than that seen in adjacent IHC areas (Robertson 1982; Liberman and Dodds 1984).

The present study is not consistent with the view that hair cells are the elements most vulnerable to irreversible noise-induced damage. In the mouse, all exposed ears showed virtually complete loss of type IV fibrocytes throughout much of the basal half of the cochlea (Fig. 12). For the 94 and 100 dB exposures, this damage was seen in the absence of other chronic light microscopic histopathology. However, for the 94 dB exposures, this widespread cell loss was associated with ABR thresholds within 5–10 dB of normal values (Fig. 12); thus, the functional consequence is limited. The extreme vulnerability of the type IV fibrocytes to noise exposure is interesting in light of the recent report that they are the first cells to degenerate in the aging C57BL/6 mouse strain, which shows an accelerated age-related hearing loss (Hequembourg and Liberman 2001). Although damage to the lateral wall fibrocytes is clearly seen in other animal models of acoustic injury, it appears in the cat ear only at exposure levels above those at which significant hair cell damage occurs (Liberman and Kiang 1978).

The widespread strial shrinkage was not expected based on previous studies. In the present study, there was significant strial shrinkage in midcochlear regions following all of the exposures (Fig. 12). This appeared to worsen monotonically with exposure level, at least to 112 dB exposures (Fig. 14). Our ultrastructural analysis of these same cases (Hirose and Liberman, unpublished) reveals extensive degeneration of intermediate cells associated with this shrinkage and decreased staining intensity visible at the light microscopic level. Thus, some diminution in the endolymphatic potential (EP) would be anticipated; indeed, previous studies have documented acute and chronic changes in EP after acoustic overexposure (Jian et al. 1990). If true, this chronic strial pathology should contribute to threshold shift as there is a close and consistent correlation between EP reduction and threshold elevation (Sewell 1984). However, in the present study, chronic shrinkage was documented after the 94 dB exposure, yet the thresholds had returned to normal (see the 8 kHz points in Fig. 14), suggesting the stria may possess excess ion-pumping capacity over what is required to maintain a normal EP at rest.

Mechanisms of noise damage

Cochlear mechanics and the tonotopic vs. hook foci of hair cell damage. Previous histopathological studies have shown that narrowband exposures often lead to two lesion foci: one near the cochlear region tuned to frequencies in the noise band and a second at or near the extreme base (hook) of the cochlea (Fried et al. 1976; Liberman and Kiang 1978; Ou et al. 2000a,b). The tonotopically appropriate lesion is usually centered about a half-octave above the stimulus frequency. This ''half-octave shift'' is consistent with nonlinear cochlear mechanics whereby the region

maximally stimulated by mid- or high-frequency tones shifts basalward as stimulus intensity increases (Cody and Johnstone 1981; Liberman and Mulroy 1982). Although the location of the hook focus is also related to exposure spectrum, the relationship is not mathematically simple, for example, because of generation of first or second harmonics. For example, in cat (Liberman and Kiang 1978), narrowband noise at 750 Hz caused punctate lesions near the 20 kHz place, whereas a band at 3.0 kHz damaged the 45 kHz place, and a 6.0 kHz band wiped out hair cells at the extreme hook (60 kHz place).

The present analysis of hair cell loss and stereocilia damage also showed discrete hook and tonotopic foci (Fig. 12). At exposure levels <116 dB SPL, our 8–16 kHz band caused hair cell loss only in the extreme cochlear base (~80 kHz place). At 116 dB, a second focus appeared in a cochlear region in the upper basal turn that was associated with rupture of the reticular lamina between the outer pillar and the first-row OHCs (Fig. 4). According to existing cochlear frequency maps, this occurs in the 6–16 kHz region (Ehret 1983) or the 5–14 kHz region (Ou et al. 2000b); however, the indirect nature of existing murine maps forces caution in assigning frequency correlates to cochlear locations. The stereocilia analysis also showed signs of the hook and tonotopic foci: At 94 and 100 dB exposures, stereocilia damage was restricted to the extreme base, whereas at 106 dB, a damage focus appears in the 8–16 kHz place.

These patterns, coupled with the present understanding of cochlear mechanics, suggest that the tonotopic focus corresponds to the cochlear region with maximal noise-induced vibration magnitude. It is not hard to imagine, for example, that the reticular lamina breach at 116 dB arises when the elastic limit of the junctional complexes at the small area of contact between pillar head is exceeded and first-row OHC and that the elastic limit of the stereocilia rootlets or tip links is exceeded at 106 dB.

On the other hand, existing cochlear physiology suggests no simple mechanical explanation for the hook focus. Measurement of the stimulus spectrum reveals no energy at these high frequencies, even when assessed within the ear canal (Liberman, unpublished). Both mechanical measurements and auditory nerve tuning curves show that high-frequency regions will respond to low-frequency stimuli (Kiang and Moxon 1974; Ruggero et al. 1986). However, thresholds on tuning-curve tails increase monotonically with increasing characteristic frequency (CF) (Liberman 1978); thus there is no reason to believe that the extreme hook is vibrating more vigorously than the rest of the lower basal turn.

These data suggest that nonmechanical explanations must be sought for the vulnerability of the hook region. For example, there is evidence for an inherent base-to-apical gradient in the susceptibility of hair cells to trauma such that hook hair cells are more easily damaged than their more apical neighbors, given the same environmental stressors. In the bird cochlea, basal hair cells are more vulnerable to ototoxic challenge *in vitro* than apical hair cells (Hirose et al. 1999), and in the mammalian cochlea, basal OHCs die more quickly *in vitro* than apical cells (Sha et al. 2001). Additional evidence for this view comes from the observation in the present study (data not shown) that there is an apex-to-base gradient in control ears in "baseline" dendritic swelling in the IHC area. Although vacuolization is clearly worsened by acoustic overexposure (Fig. 13), these signs of "damage" were increasingly difficult to eliminate from "normal" ears with increasing proximity to the base. This control gradient in vacuolization suggests that basal cochlear regions are particularly vulnerable to the hypoxia which precedes tissue fixation during intravascular perfusion.

Another potential contributor to the vulnerability of the lower basal turn is its proximity to the round window membrane. This proximity greatly decreases the volume of scala tympani. This volume decrease, which is especially striking in the mouse, could decrease the capacity of the perilymph spaces to quickly dilute metabolites released by the sensory epithelium, e.g., reactive oxygen species, which could have deleterious effects on the hair cells.

Complementary lesion foci: "protective" effects of hair cell damage? Several cell types showed longitudinal patterns of tissue damage which were complementary to the hook and tonotopic foci seen for hair cell and supporting cells. The most robust of these patterns was shared by ligament fibrocytes (Fig. 12) and vacuolization in the IHC area and the spiral ganglion (Fig. 13). Each of these structures showed a damage focus that spanned the regions between the hook and tonotopic foci, i.e., it was complementary to the foci of hair cell damage. Strict complementarity between loci of hair cell loss and spiral ligament pathology has been noted in previous studies of permanent noise-induced histopathology in the cat ear (Liberman and Kiang 1978). In the cat study, the spiral prominence (the major site of type II fibrocytes) was atrophic in regions both apical and basal to (but not within) the midcochlear tonotopic focus of hair cell and supporting cell loss (Liberman and Mulroy 1982).

One interpretation of this complementarity of damage foci is that damage to some cell types occurs secondarily to processes requiring transduction and synaptic transmission of the acoustic overexposure (rather than to the acoustic overexposure itself), such as accumulation of released glutamatergic transmitters or excessive K^+ fluxes. Thus, local accumulation

of hair cell damage during the acoustic overexposure may serve to minimize the development of some other cellular pathologies in the same cochlear regions by shutting down transduction and/or transmission.

Consider first the pathology of neuronal swelling since mechanisms underlying its generation are better understood (for review, see Pujol and Puel 1999). The swelling of afferent dendrites under IHCs can be mimicked by cochlear perfusion of glutamate receptor agonists such as kainate (Ruel et al. 2000). Pharmacological studies suggest that this excitotoxicity is mediated by AMPA-type receptors (Ruel et al. 2000), which are expressed by both cochlear and vestibular neurons (Niedsielski and Wenthold 1995). In the present study, vacuolization in the IHC area (Fig. 13) was associated, at slightly later postexposure times (Fig. 16), with swelling of cells in the spiral ganglion. The similarity of our light microscopic images with those of cochlear ganglion cells exposed to kainate (Sun et al. 2001) is consistent with glutamate excitotoxicity. At the ultrastructural level, the vacuoles were shown to be within the satellite cells. Although swelling in satellite cells could arise secondarily to excitotoxic effects on the neurons, a direct effect is also possible given that (1) the satellite cells are immunopositive for a number of glutamate receptors [both AMPA and NMDA type - (Niedsielski and Wenthold 1995)] and (2) glutamate in perilymph should have access to the extracellular spaces around the ganglion cells. In this context, it is interesting that the satellite cells are also positive for GLAST, a glial glutamate transporter implicated in the control of glutamate concentration in the noise-exposed ear (Hakuba et al. 2000). In a GLAST knockout mouse, perilymphatic glutamate levels rise dramatically after acoustic overexposure (whereas they do not in wild-type mice).

Given that vacuolization is an excitotoxic effect related to glutamatergic synaptic transmission and that synaptic transmission in all cochlear regions basal to the 8 kHz place will initially be strongly driven by the exposure stimulus, the entire basal turn should be at risk for vacuolization phenomena. However, development of stereocilia damage during the acoustic exposure and the fact that it is first seen (with increasing exposure intensity) in the tonotopic and hook foci could result in a vacuolization pattern which tends to exclude foci of hair cell damage due to the reduction in transduction/synaptic transmission in those areas.

By this reasoning, a complementary damage pattern would be expected for any ''downstream'' effect of processes requiring transduction and synaptic transmission for its development. Thus, the damage to both type II and type IV fibrocytes in the spiral ligament may occur secondarily to excessive K^+ flux through transduction channels or excessive production of glutamate or its analogs by IHCs. The idea that damage to the transduction apparatus, i.e., stereocilia, could locally reduce excessive K^+ flux during an acoustic overexposure is intriguing in light of the observation that both type II and type IV fibrocytes express a number of ion transporters including the Na^+/K^+-ATPase and the $Na^+/K^+/Cl^-$ cotransporter and that both cell types have been implicated in the recycling of K^+ back to the stria vascularis (Spicer and Schulte 1991). It is possible that sound-induced K^+ overload leads to degeneration of these cell types. Correspondingly, the idea that glutamate excitotoxicity might be reduced in tonotopic and hook foci is intriguing in light of the facts that (1) the glutamate transporter GLAST is present in the spiral ligament in the region rich in type II fibrocytes (Hakuba et al. 2000) and (2) glutamate receptors are also seen on ligament fibrocytes, at least during development (Luo et al. 1995).

Excitotoxicity and "protective" effects of reticular lamina rupture. Our quantitative analyses (Fig. 15) revealed that average prevalence of satellite cell swelling behaved nonmonotonically with exposure level, with significantly fewer cells affected at 116 dB than at lower SPLs, especially near the tonotopic focus (8.0 kHz points in Fig. 15). Data from individual animals (not shown) strongly suggested that the reticular lamina rupture itself was the determinant rather than exposure level *per se,* i.e., among ears evaluated at 24 h postexposure, the one case at 116 dB that did NOT rupture showed cell swelling comparable to that among the 112 dB cases (none of which showed ruptures), whereas three cases at 116 dB in which the lamina was ruptured all showed few affected cells compared with that seen at lower exposure levels.

There are a number of mechanisms whereby reticular lamina rupture could reduce these transient excitotoxic effects. (1) A breach of the endolymph/perilymph barrier would stop transduction and associated release of glutamatergic transmitters from hair cells in the immediate vicinity. (2) The associated reduction in endolymphatic potential could also reduce transduction and associated release of glutamatergic substances in areas within 1–2 space constants of the breach [corresponding to several millimeters of cochlea length (Johnstone et al. 1966)] (3) Mixing of endolymph into perilymph could reduce Na^+ and Ca^{2+} concentration surrounding the satellite cells and thereby reduce the Ca^{2+} and Na^+ entry involved in the development of excitotoxicity through glutamate receptor channels (for review, see Sattler and Tyminaski 2000).

The present results strongly suggest that limbus fibrocytes are also ''protected'' when the reticular

lamina ruptures (Figs. 12 and 14). As for satellite cell swelling, a case-by-case correlation between presence of lamina rupture and protection of limbic fibrocytes was seen among the 116 dB cases. By analogy to the nonmonotonicity with exposure level in the satellite cell pathology, it is possible that the limbic degeneration also represents an excitotoxic effect. The case is not compelling since so little is known about these fibrocytes; however, the fact that they, like the satellite cells, are strongly positive for GLAST (Hakuba et al. 2000) as well as for various NMDA glutamate receptors (Luo et al. 1995) makes the possibility worth considering. One obvious test would be to assess the effects of perfusion of glutamate receptor agonists on the limbus. However, in our acoustic injury model, limbic degeneration was not clearcut until 1 weeks postexposure, and cochlear perfusion experiments have typically been acute. Degeneration of limbic central zone fibrocytes, with selective sparing of the interdental cells, is not unique to the mouse. Limbic degeneration patterns very similar to that seen here have been reported as a permanent histopathology following narrowband noise exposures in the cat (Liberman and Kiang 1978).

Mechanisms and time course of hair cell and supporting cell loss. The distinction between hook and tonotopic foci of damage is important when considering possible mechanisms of hair cell and supporting cell damage because the mechanisms are probably very different in these two regions, possibly reflecting the type of fundamental distinction between metabolic and mechanical effects originally suggested by Spoendlin (1971).

In the chronic ear, the hook focus consisted of selective OHC loss with sparing of IHCs and all supporting structures. The selective loss of basal OHCs is also seen *in vitro*, where it can be significantly ameliorated by addition of radical-scavenging antioxidants (Sha et al. 2001). Thus, one simple view is that the hook lesion arises from ''metabolic'' effects mediated via accumulation of reactive oxygen species. In contrast, the tonotopic focus resolved in the chronic state to areas with total loss of all hair cells as well as most of the supporting structures of the organ of Corti. Given that this type of massive cellular loss arose only at 116 dB and only at 116 dB was there acute rupture of the reticular lamina, it is tempting to speculate that wipeout of the organ of Corti arises only after reticular lamina breach. Such a breach allows mixing of endolymph and perilymph, which could lead to a rapid and massive cell death via either (1) an increase in the K^+ concentration bathing the basolateral surfaces of the hair cells [as suggested by Bohne and Rabbit (1983)] or (2) an increase in Na^+ and Ca^{2+} bathing the apical surfaces of epithelial cells designed to be in contact with the low Na^+ and low Ca^{2+} of endolymph. These breaches in the reticular lamina were still patent 1 week postexposure but never at 2 weeks or later; thus, the ill effects of fluid mixing can persist for many days. Thus, one simple view of damage mechanisms for the tonotopic focus is that the hair cell loss here arises fundamentally via mechanical disruption of fluid barriers.

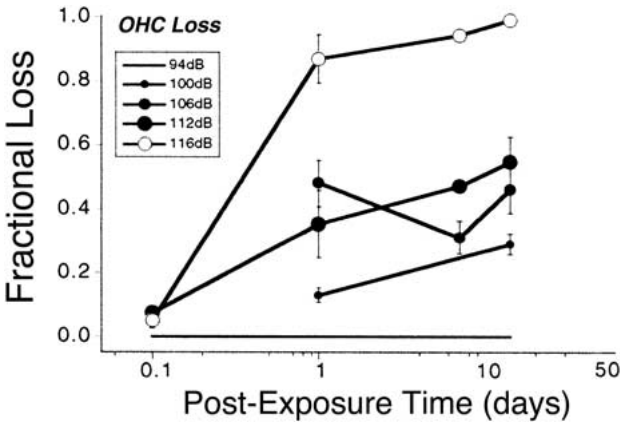

FIG. 17. The continued loss of OHC with postexposure time from 0 h to 2 weeks data are compiled separately for each of the five noise exposure groups.

The support structure changes in the hook focus were much less dramatic. Immediately after the noise exposure (0–24 h), there was widespread swelling of OHC nuclei (Fig. 2) with little loss of hair cells apparent until 24 h (Fig. 17). This was especially prevalent at 116 dB exposures in all cochlear regions basal to that at which the reticular lamina was ruptured. According to our analyses, swelling of OHC nuclei is the acute manifestation of OHCs that will go on to degenerate, as this phenomenon was seen only at 0 and 24 h and only in cochlear regions that were destined to lose all OHCs.

The most significant OHC loss occurred within the first 24 h (Fig. 17), at which time there was appreciable cellular debris in the OHC area. A scanning electron microscopic study of this type of selective OHC loss suggests that "holes" appear in the reticular lamina where OHC cuticular plates used to be (Bohne and Rabbitt 1983). Our ultrastructural analysis suggested that such holes remained "plugged" by cuticular plates even after the OHC membranes were massively disrupted and the cytoplasm apparently dispersed (data not shown). At none of the exposures or postexposure survivals did we see a significant number of apoptotic figures in the OHC area, i.e., shrunken cells with intact membranes enclosing nuclei with condensed or fragmented chromatin, although they were common in the spiral ligament and stria vascularis at the 0- and 24-h survivals. Thus, if apoptotic hair cell degeneration occurs in the noise-

damaged mouse ear, it must peak between 0 and 24 h (and thereby have evaded our analysis).

Regardless of the balance of necrosis and apoptosis in the genesis of hair cell loss in the mouse ear, the present study provides strong evidence that significant hair cell loss in the hook focus continues for at least 2 weeks after the noise exposure. As such, this suggests that post-trauma pharmacological intervention could significantly enhance hair cell survival as the degenerative mechanisms are better clarified.

Summary of results

- Hearing loss and cellular damage were quantified in noise-exposed CBA/CaJ mice to assess the dynamics of tissue injury and repair over a wide range of exposure levels, from those causing severe TTS to those causing profound PTS.
- Hair cell loss and stereocilia damage after narrowband exposure occurred in two foci: one tonotopically appropriate, the other in the extreme base (hook).
- The hook focus often showed selective OHC death, which spread apically with increasing exposure level. Most OHC death occurred within 24 h; however, significant loss continued for at least 2 weeks. Cochlear mechanics provides no explanation for a hook damage focus; however it may arise from intrinsic gradients in antioxidant abilities from apex to base.
- The tonotopic focus typically resolved in the chronic state to a region of complete loss of the organ of Corti. In the acute state, there was gross mechanical disruption of the reticular lamina between outer pillar and first-row OHC. These changes were seen only at the highest exposure level: 116 dB.
- Stereocilia damage was seen immediately after the exposure. There was no evidence for recovery, and, at 2 weeks postexposure, the pattern of stereocilia damage was the best predictor of the degree and pattern of PTS. By contrast, profound levels of PTS were routinely seen in the absence of any significant hair cell loss (outside of the hook focus).
- Acute changes in the organ of Corti also included collapse of the Hensen cells and the outer space of Nuel. This collapse may affect cochlear micromechanics and thus contribute to both TTS and PTS. These changes were seen immediately after exposure and showed significant recovery over the same time course that significant TTS recovery was observed.
- Acute pathology in neural structures included terminal swelling in the IHC area and swelling of satellite cells in the spiral ganglion. The cochlear location of these putative excitotoxic changes was complementary to that of hair cell damage (spanning the region between the hook and tonotopic foci), suggesting that hair cell damage and the resultant decrease in transmitter release during the sound exposure may protect neural structures. Swelling of cells in the ganglion was also apparently reduced by rupture of the reticular lamina.
- The spiral ligament showed focal loss of type IV fibrocytes by 2 weeks after all exposures, including 94 dB, at which level thresholds had returned to near-normal values. As for excitotoxic effects, the longitudinal pattern was complementary to hair cell loss.
- The limbus showed chronic fibrocyte loss near the tonotopic focus. This histopathology grew with increasing exposure level but was strikingly reduced at the highest levels, in which there was nearby rupture of the reticular lamina.
- The stria vascularis showed acute swelling throughout the cochlea, peaking at 24 h, reversing by 1 week, and resolving to a shrunken state at 2 weeks. Acute swelling and chronic shrinkage increased monotonically with increasing exposure level and may reflect K^+ accumulation in the intrastrial space due to increased K flux through transduction channels.
- Noise-induced damage in the mouse cochlea can be seen in a wide range of cochlear cell types. Marked differences in the spatial distribution, time course, and level dependence of these pathologies is suggestive of complex interactions among these cell types in which increasing damage in one structure can decrease the damage in other structures.

ACKNOWLEDGMENTS

This work was supported by NIDCD Grant No. RO1 DC0188.

REFERENCES

BOHNE BA, HARDING GW, NORDMANN AS, TSENG CJ, LIANG GE, BAHADORI RS. Survival fixation of the cochlea: a technique for following time dependent degeneration in noise-exposed chinchillas. Hear. Res. 123:162–178, 1999.

BOHNE BA, RABBITT KD. Holes in the reticular lamina after noise exposure: Implication for continuing damage in the organ of corti. Hear. Res. 11:41–53, 1983.

CODY AR, JOHNSTONE BM. Acoustic trauma: single neuron basis for the "half-octave shift." J. Acoust. Soc. Am. 70(3):707–711, 1981.

EHRET G. Peripheral anatomy and physiology II. In Willott JF (ed) The Auditory Psychobiology of the Mouse. Springfield, IL, Charles C. Thomas, pp 169–200, 1983.

FLOCK A, FLOCK B, FRIDBERGER A, SCARFONE E, ULFENDAHL M. Supporting cells contribute to control of hearing sensitivity. J. Neurosci. 19(11):4498–4507, 1999.

FRIED MP, DUDEK SE, BOHNE BA. Basal turn cochlear lesions following exposure to low-frequency noise. Trans. Am. Acad. Ophthalmol. Otolaryngol. 82:285–298, 1976.

HAKUBA N, KOGA K, GYO K, USAMI S, TANAKA K. Exacerbation of noise induced hearing loss in mice lacking the glutamate transporter GLAST. J. Neurosci. 20(23):8750–8753, 2000.

HEQUEMBOURG SJ, LIBERMAN MC. Spiral ligament pathology: a major aspect of age-related cochlear degeneration in C57BL/6J mice. J. Assoc. Res. Otolaryngol. 2:118–129, 2001.

HIROSE K, WESTRUM LE, STONE JS, ZIRPEL L, RUBEL EW. Dynamic studies of ototoxicity in mature avian auditory epithelium. Ann. N. Y. Acad. Sci. 884:389–409, 1999.

HUSBANDS JM, STEINBERG SA, KURIAN R, SAUNDERS JC. Tip link integrity on chick tall hair cells stereocilia following intense sound exposure. Hear. Res. 135:135–145, 1999.

JIAN W, WEI-JIA D, JI-SHENG C. Changes in endocochlear potential during anoxia after intense exposure. Hear. Res. 44:143–150, 1990.

JOHNSTONE BM, JOHNSTONE JR, PUGSLEY LD. Membrane resistance in endolymphatic walls of the first turn of the guinea pig cochlea. J. Acoust. Soc. Am. 40:1398–1404, 1966.

KIANG NYS, MOXON EC. Tails of tuning curves of auditory-nerve fibers. J Acoust. Soc. Am. 55(3):620–630, 1974.

LIBERMAN MC. Auditory-nerve response from cats raised in a low-noise chamber. J. Acoust. Soc. Am. 63(2):442–455, 1978.

LIBERMAN MC, CHESNEY CP, KUJAWA SG. Effects of selective inner hair cell loss on DPOAE and CAP in carboplatin-treated chinchillas. Aud. Neurosci. 3:255–268, 1997.

LIBERMAN MC, DODDS LW. Single-neuron labeling and chronic cochlear pathology. III Stereocilia damage and alterations of threshold tuning curves. Hear. Res. 16:55–74, 1984.

LIBERMAN MC, DODDS LW. Acute ultrastructural changes in acoustic trauma: serial-section reconstruction of stereocilia and cuticular plates. Hear. Res. 26:45–64, 1987.

LIBERMAN MC, KIANG NYS. Acoustic trauma in cats, cochlear pathology and auditory-nerve activity. Acta Otolaryngol. 358:5–63, 1978.

LIBERMAN MC, MULROY MJ. Acute and chronic effects of acoustic trauma: Cochlear pathology and auditory nerve pathophysiology. In: Hamernik RP, Henderson D, Salvi R (eds) New Perspectives on Noise-Induced Hearing Loss. New York, Raven Press; pp. 105–136, 1982.

is erf a book? if so, pls provide city and name of publisher

LUO L, BRUMM D, RYAN AF. Distribution of non-NMDA glutamate receptor mRNAs in the developing rat cochlea. J. Comp. Neurol. 361:372–382, 1995.

MAISON SF, LIBERMAN MC. Predicting vulnerability to acoustic injury with a non-invasive assay of olivocochlear reflex strength. J. Neurosci. 20:4701–4707, 2000.

MULROY MJ, WHALEY EA. Structural changes in auditory hairs during temporary deafness. Scan. Electron Microsc. II:831–840, 1984.

NIEDSIELSKI AS, WENTHOLD RJ. Expression of AMPA kainate and NMDA receptor subunits in cochlear and vestibular ganglia. J. Neurosci. 15(3):2338–2353, 1995.

NORDMANN AS, BOHNE BA, HARDING GW. Histopathological differences between temporary and permanent threshold shift. Hear. Res. 139:13–30, 2000.

OHLEMILLER KK, MCFADDEN SL, DING DL, FLOOD DG, REAUME AG, HOFFMAN EK, SCOTT RW, WRIGHT JS, PUTCHA GV, SALVI RJ. Targeted deletion of the cytosolic Cu/Zn-superoxide dismutase gene (Sod1) increases susceptibility to noise-induced hearing loss. Audiol. Neurootol. 4:237–246, 1999.

OU HC, BOHNE BA, HARDING GW. Noise damage in the C57B1/CBA mouse cochlea. Hear. Res. 145:111–122, 2000a.

OU HC, HARDING GW, BOHNE BA. An anatomically based frequency place map for the mouse cochlea. Hear. Res. 145:123–129, 2000b.

PUEL JL, BOBBIN, RP, FALLON M. The active process is affected first by intense sound exposure. Hear. Res. 37:53–64, 1988.

PUJOL R, PUEL JL. Excitotoxicity, synaptic repair and functional recovery in the mammalian cochlea: a review of recent findings. Ann. N. Y. Acad. Sci. 884:249–254, 1999.

ROBERTSON D. Effects of acoustic trauma on stereocilia structure and spiral ganglion cell tuning properties in the guinea pig cochlea. Hear. Res. 7:55–74, 1982.

ROBERTSON D. Functional significance of dendritic swelling after loud sounds in the guinea pig cochlea. Hear. Res. 9:263–278, 1983.

RUEL J, BOBBIN RP, VIDAL D, PUJOL R, PUEL JL. The selective AMPA receptor antagonist GYKI 5387 blocks action potential generation and excitotoxicity in the guinea pig cochlea. Neuropharmacology 39:1959–1973, 2000.

RUGGERO MA, ROBLES I, RICH NC. Basilar membrane mechanics at the base of the chinchilla cochlea. II. Responses to low-frequency tones and relationship to microphonics and spike initiation in the VIII nerve. J. Acoust. Soc. Am. 80(5):1375–1383, 1986.

SANTI PA, DUVALL AJ. Stria vascularis pathology and recovery following noise exposure. ORL J. Otorhinolaryngol. Relat. Spec. 86(2):354–361, 1978.

SATTLER R, TYMINASKI M. Molecular mechanisms of calcium-dependent excitotoxicity. J. Mol. Med. 78:3–13, 2000.

SAUNDERS JC, DEAR SP, SCHNEIDER ME. The anatomical consequences of acoustic injury: A review and tutorial. J. Acoust. Soc. Am. 78(3):833–860, 1985.

SEWELL WF. The effects of furosemide on the endocochlear potential and auditory-nerve fiber tuning curves in cats. Hear. Res. 14:305–314, 1984.

SHA SH, TAYLOR R, FORGE A, SCHACHT J. Differential vulnerability of basal and apical hair cells is based on intrinsic susceptibility to free radicals. Hear. Res. 155:1–8, 2001.

SPICER SS, SCHULTE BA. Differentiation of inner ear fibrocytes according to their ion transport related activities. Hear. Res. 56:53–64, 1991.

SPOENDLIN HH. Primary ultrastructural changes in the organ of Corti after acoustic overstimulation. Acta Otolaryngol. 71:166–176, 1971.

SUN H, HASHINO E, DING DL, SALVI RJ. Reversible and irreversible damage to cochlear afferent neurons by kainic acid excitotoxicity. J. Comp. Neurol. 430:172–181, 2001.

YOSHIDA N, HEQUEMBOURG SJ, ATENCIO CA, ROSOWSKI JJ, LIBERMAN MC. Acoustic injury in mice: 129/SvEv is exceptionally resistant to noise-induced hearing loss. Hear. Res. 141:97–106, 2000.

YOSHIDA N, LIBERMAN MC. Heat stress and protection from acoustic injury in Mice. J. Neurosci. 19:10116–10124, 1999.

YOSHIDA N, LIBERMAN MC. Sound conditioning reduces noise-induced permanent threshold shift in mice. Hear. Res. 148:213–219, 2000.

ZHAO Y, YAMOAH EN, P.G.G. Regeneration of broken tip links and restoration of mechanical transduction in hair cells. Proc. Natl. Acad. Sci. 93(26):15469–15474, 1996.

ZHENG XY, HENDERSON D, HU BH, MCFADDEN SL. Recovery of structure and function of inner ear afferent synapses following kainic acid excitotoxicity. Hear. Res. 105:65–76, 1997.